REALIZATION OF OTA BASED SHADOW FILTERS

A PROJECT REPORT

SUBMITTED IN PARTIAL FULFILLMENT OF THE REQUIREMENTS
FOR THE AWARD OF THE DEGREE
OF

MASTER OF TECHNOLOGY
IN
VLSI DESIGN AND EMBEDDED SYSTEM

Submitted by:

CHAUDHARY SHIKHA
2K16/VLS/07

Under the supervision of

PROF. NEETA PANDEY

DEPARTMENT OF ELECTRONICS AND COMMUNICATION ENGINEERING
DELHI TECHNOLOGICAL UNIVERSITY
(Formerly Delhi College of Engineering)
Bawana Road, Delhi-110042

MAY, 2018

DEPARTMENT OF ELECTRONICS AND COMMUNICATION ENGINEERING
DELHI TECHNOLOGICAL UNIVERSITY
(Formerly Delhi College of Engineering)
Bawana Road, Delhi-110042

CANDIDATE'S DECLARATION

I, Chaudhary shikha, Roll No. 2K16/VLS/07 student of M.Tech. (VLSI DESIGN AND EMBEDDED SYSTEM), hereby declare that the project Dissertation titled **"NEW OTA BASED VOLTAGE MODE SHADOW FILTERS"** which is submitted by me to the Department of ELECTRONICS AND COMMUNICATION ENGINEERING, Delhi Technological University, Delhi in partial fulfillment of the requirement for the award of the degree of Master of Technology, is original and not copied from any source without proper citation. This work has not previously formed the basis for the award of any Degree, Diploma Associate ship, Fellowship or other similar title or recognition.

Place: Delhi **CHAUDHARY SHIKHA**
Date:

DEPARTMENT OF ELECTRONICS AND COMMUNICATION ENGINEERING

DELHI TECHNOLOGICAL UNIVERSITY

(Formerly Delhi College of Engineering)

Bawana Road, Delhi-110042

CERTIFICATE

I hereby certify that the Project Dissertation titled **"A NEW OTA BASED VOLTAGE MODE SHADOW FILTERS"** which is submitted by CHAUDHARY SHIKHA, Roll No 2K16/VLS/07 Department of Electronics And Communication Engineering, Delhi Technological University, Delhi in partial fulfillment of the requirement for the award of the degree of Master of Technology, is a record of the project work carried out by the students under my supervision. To the best of my knowledge this work has not been submitted in part or full for any Degree or Diploma to this University or elsewhere.

Place: Delhi

Date:

PROF. NEETA PANDEY

SUPERVISOR

ACKNOWLEDGEMENT

I express my deepest gratitude to my supervisor, Prof. Neeta Pandey, Department of Electronics and Communication Engineering, DTU. Whose encouragement, guidance and support from the initial to the final level enabled me to develop an understanding of the subject. Her suggestions and ways of summarizing the things made me to go for independent studying and trying my best to get the maximum in my topic, this made my circle of knowledge very vast. I attribute the level of my Masters degree to her encouragement and effort and without her this thesis, too, would not have been completed or written. I am highly thankful to her for guiding me in this project.

I am also grateful to Prof. S. Indu, HOD, Department of Electronics and Communication Engineering, DTU for her immense support. I would also acknowledge DTU for providing the right academic resources and environment for this work to be carried out.

Finally, I take this opportunity to extend my deep appreciation to my family and friends, for all that they meant to me during the crucial times of the completion of my project.

Date

Chaudhary Shikha

2K16/VLS/07

M.Tech (VLSI Design and Embedded System)

ABSTRACT

Shadow filter is a second order filter in which an external amplifier is placed in the feedback path and the characteristics of such a filter are tuned by adjusting the gain (G) of the external amplifier. New voltage-mode electronically tunable band pass, notch, high pass and low pass shadow filters are proposed. The filters are built around the operational transconductance amplifier (OTA). OTA provides an electronic tuning capability of its transconductance gain by adjusting its bias current or voltage and is implemented by using the CMOS technology. The circuits implemented by using the OTA does not require a resistor which is ideal for any of the integrated circuit Implementation. In every case one or more than one parameters of the filters can be electronically controlled by adjusting the gain of an external amplifier built around the operational transconductance amplifier. The proposed circuit has utilized the MISO configuration, avoiding the external summing amplifier for implementing the shadow filter. For realizing the filter functions, there is no need of the component-matching conditions. The proposed shadow filter is simulated using SPICE simulator with 0.35 μm CMOS process from TSMC to confirm the presented theory.

TABLE OF CONTENTS

LIST OF FIGURES

LIST OF ABBREVIATIONS

Abbreviation	Full Form
CMOS	Complementary Metal Oxide Semiconductor
BJT	Bipolar Junction Transistor
Op-Amp	Operational Amplifier
IC	Integrated Circuit
AC	Alternating Current
DC	Direct Current
VLSI	Very Large Scale Integration
ADC	Analog to Digital Convertor
DAC	Digital to Analog Convertor
CM	Current Mode
VM	Voltage Mode
CFOA	Current Feedback Operational Amplifier
OTA	Operational Transconductance Amplifier
TA	Transconductance Amplifier
CC	Current Conveyor

CCII	2nd generation Current Conveyor
CCTA	Current Conveyor Transconductance Amplifier
DDCC	Differential Difference Current Conveyor
B.W.	Bandwidth
H P	High Pass filter
L P	Low pass filter
B P	Band pass filter
B S	Band Stop filter

CHAPTER 1

INTRODUCTION

1.1. BACKGROUND

This is a digital age and everything around uses extensively digital components such as digital computers, digital communications, digital broadcasting. Though digital system has many advantages over analog systems but there is need to interface these with the real analog world. For example, the digital signal processing offers advantage only if it's processing takes place on bandlimited signals if unwanted aliasing effects are not to be introduced. After processing the signals are returned to the real analog world after passing to the reconstruction filter. Both bandlimited and reconstruction filters are the analog filters, which operates in continuous time. Any system that interfaces with the real world will found use of continuous time filters [1].

There was a time when analog filters were used to process analog signals in real time, compared to digital which performs filtering operations on digital representation of samples of signals, often not in real time. Then in 1970s sampled data filters were introduced. Sampled data filters did not work with digital representations of sampled signals but operate on the samples themselves. The best example of this approach is switched capacitor filter which uses switches along with the capacitors and active devices for filtering operation. These filters are discontinuous in time due to switching which takes place in these circuits. So continuous band limited and reconstruction filters were needed as a result [1]. Due to the advantages for integrated circuit realization provided by the switched capacitor filters much research was done in 1970s, 1980s on them. But when capacitor filters failed to provide all the solutions traditional approaches started getting attention and the name continuous time filter was coined to distinguish them from their digital and sampled data counterparts.

The classic LCR filters which uses inductors, capacitors and resistors are much in use but these filters are not suitable for implementation of the ubiquitous integrated circuits because no satisfactory method for making inductors on chip has been found [1]. This is the reason that the active continuous time filters have found so much attention over the years. The active filters provide an opportunity to integrate complex filters on chip and also do not have the problem that bulky, lossy and expensive filters have.

Active filters have been around for some time to overcome the disadvantages of the passive filters. The Sallen and Key is active RC filter and is popular and are in existence for more than 40 years. It uses voltage amplifier, resistors, and capacitors. But research on active filters continues for all the time and thousands of research papers have been published on the same over the years. There are so many reasons for this but in particular two reasons are of note. First due to changes in the technology there is need of new approach so the cheap and easily available OP-AMP replaced their discrete circuits' counterparts. So it became possible to realize the filter circuits using large numbers of OP-AMPs and we get new improved architecture. In the same way development of operational transconductance amplifier also called as OTA led to new filter configurations. Second, the demand on filter circuit has become more stringent as the world of electronics and communications have advanced. The OTA is an important basic building block that is used in many analog circuits with linear input-output characteristics. The operational trans-conductance amplifier (OTA) is an amplifier which produces an output current with differential input voltage. Thus, it can be concluded that it is a voltage controlled current source (VCCS). The OTA uses an additional input current known as amplifier bias current, denoted by $I_{abc}$to control the amplifier's trans-conductance. This property makes OTA useful for electronic control of amplifier gain. The OTA has high impedance differential input stage like operational amplifier and thus it can be used with negative feedback. The OTA is easily available, low price device and it is having all the attractive features of an OP-AMP. As OTA is a programmable device and has only one high-impedance node, this makes OTA an important device in high frequency and programmable building block. The circuits implemented by using OTA do not require resistor which is ideal for any of the integrated circuit implementation. A variety of papers have been reported on electronically tunable universal filters [2-4] using OTAs in last few decades. The continuous increase in the operating frequency of modern circuits reflects on in need of active filters which can operate on these higher frequencies in an area where OTA active filters outshines its active RC counterpart. The OTA-based filter consumes very low power since it can be biased in weak inversion.

Active band pass filter based on OTA using simple CMOS current mirrors is presented in [5]. It uses an active inductor that is made from OTA circuits [6]. The OTA based AP filters without resistor connection have been introduced in [7]. This paper also includes fully tunable all-pass (AP) filter design and its application. First order all-pass filter using OTAs with single/dual outputs and grounded capacitors has been put forward [8]. A new

electronically tunable voltage-mode first-order all pass filter using only three single-ended operational transconductance amplifiers (OTAs) and one grounded capacitor is presented in [9], which is highly suitable for integrated circuit implementation. The OTA-C approach is one of the most successful design methods for continuous-time integrated filter design at high frequencies. The term OTA-C filters was first used in [10] in terms of C-OTA filters. Another important OTA-C filter is presented in [11], where versatile filter functions were achieved by switches. A novel, multifunction, universal high frequency biquadratic filter using dual output OTA is presented [12]. By programming the input nodes, different types of second order filters are realized in [12]. Digitally programmable OTA-based integrators and differentiators have been presented in [13]. Novel voltage attenuation technique based on the network of nonlinear OTAs for Gm reduction which can extend the input linear range of the OTA, and achieve very low Gm and lower noise is presented in [14]. Digital programmable balanced OTA employing three linearization techniques which are the source degeneration, double differential pair (DDP) and the adaptive biasing has been presented in [15].A new approach to implement a multiphase sinusoidal oscillator using loop-back of n-cascaded high-pass filters form has been presented in [16]. Gain and frequency response of high-pass filter can be independently tuned through the particular bias current.

A new method for electronic tuning of the filter parameters has been implemented in a recently proposed family of second-order filters [17] known as the shadow filters. In this type of filters an external amplifier is needed in the feedback path and the characteristics of such a filter are tuned by adjusting the gain (A) of the external amplifier. The concept of shadow filter is becoming very popular [17]-[27]. This is because of its ability of modifying the various parameters of the filters; for example the bandwidth, over a wide range by only adjusting the gain from outside of the filter and without creating disturbance of any active and passive component of the filter. However the hop between the two continuous center frequencies will become very fast. The theory of shadow filter can be applied to voltage-mode or the current-mode circuits. The shadow filter has been implemented by using various blocks like second generation current controlled conveyor (CCCII), operational transresistance amplifier (OTRA), differential difference current conveyor (DDCC) etc but it has not been implemented using OTA. A new OTA based voltage mode shadow filter has been proposed in this thesis. This proposed shadow filter has the advantage that for realizing the filter functions, there is no need of component-matching conditions and it also eliminates the need of summing amplifier which is required in current mode shadow filters.

1.2. OBJECTIVE

In the view of the discussion provided above, the thesis has focused on the following objectives for making voltage-mode OTA-based shadow filter:

• Study and characterization of OTA

• Study and implementation of OTA based applications

• Development of OTA based shadow filter structure

All simulations are done through PSPICE simulators with 0.35 µm CMOS process from TMSC.

1.3. ORGANIZATION OF THESIS

Chapter 1: Presents the brief introduction of the filters and their importance for the operation of various electronic circuits. This chapter also discusses the motivation and objective of the work undertaken.

Chapter 2: Presents brief introduction of OTA and it is also studied and simulated. It is also characterized for DC, AC and transient responses and various performance parameters are extracted through simulations.

Chapter 3: Some existing applications of OTA are implemented and verified. The applications include differentiator, integrator, divider, multiplier and multi-input single-output voltage-mode Universal filter.

Chapter 4: An extensive survey of shadow filters literature and its structure and survey of various multi-input ingle-output voltage-mode universal filters using OTAs.

Chapter 5: A new structure of single-feedback shadow filter is proposed and also various configurations of single-feedback shadow filters like band pass shadow filter, high pass shadow filter and band pass shadow filter are also implemented and simulated to verify the simulation results with the theoretical values. The filter responses are simulated to validate the workability of the proposed filter.

Chapter 6: A new structure of two-feedback shadow filter is proposed. A new two-feedback multi-input single-output voltage-mode shadow notch filter is also proposed, implemented and simulated to verify the simulation results with the theoretical values. The filter responses are simulated to validate the workability of the proposed filter

Chapter 7: This chapter summarizes the work presented in this thesis and also the future work has been discussed.

CHAPTER 2

OPERATIONAL TRANSCONDUCTANCE AMPLIFIER

This Chapter describes preliminaries related to the OTA. The OTA symbol, terminal characteristics are presented first and are followed by its characterization. The present work uses OTA as an active block for developing different filter circuits.

2.1. THE OTA

The operational transconductance amplifier (OTA) is an amplifier which produces an output current with differential input voltage. Thus it behaves as a voltage controlled current source (VCCS). In OTA there is an additional input current known as amplifier bias current, denoted by $I_{abc}$to control the amplifier's transconductance. This property makes OTA useful for electronic control of amplifier gain. OTA is easily available, low price device and it is having all the attractive features of an .operational amplifier. OTA is a programmable device and has only one high-impedance node, this makes OTA an important device in high frequency and programmable building block. Thus, the implementation of various analog circuits using only OTA as standard cell will be easily constructed from easily available cells, and also will simplify the design and the layout. OTA provides an electronic tuning capability of its transconductance gain by adjusting its bias current or voltage and can be implemented" by using both bipolar and CMOS technologies. The circuit implemented by using the OTA does not .require a resistor which is ideal for any of the integrated circuit implementation.

In an ideal OTA, the output current is a linear function of the differential input voltage, and it is expressed by an equation:

$$"I_{out} = (V_1 - V_2).g_m" \qquad (2.1)$$

Where $V1$ is the voltage at the non-inverting input, $V2$ is the voltage at the inverting input and g_m is the transconductance of the amplifier. The symbol of an operational transconductance amplifier is shown in Fig.2.1.

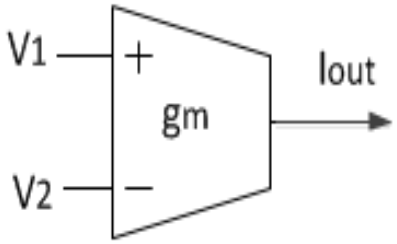

Fig.2.1. OTA Symbol

2.2. OTA CHARACTERIZATION

The CMOS implementation of the OTA is shown in Fig.2.2 [36] which consists of four transistors. $M_1 - M_2$ are the NMOS transistors and $M_3 - M_4$ are the PMOS transistors as shown in Fig.2.2. The transistors $M_1 - M_2$ are matched and .operate in saturation region and transistors $M_3 - M_4$.are also perfectly matched, the transconductance (g_m).can be expressed .as

$$g_m = \sqrt{\mu c_{ox} \left(\frac{W}{L}\right) I_{abc}} \qquad (2.2)$$

Where I_{abc} is.the biasing current,.μ is the .carrier mobility, Cox. is the gate. Oxide capacitance per unit area, W and L .are the channel width and length respectively of the .transistors M1, M2, M3 and M4. VDD and VSS are the supply voltages. The OTA circuit in Fig.2.2 is simulated with 0.35 μm CMOS process from TSMC. The aspect ratio of transistors is W/L=10μm/1μm for PMOS devices and W/L=5μm/1μm for NMOS devices. The biasing currents of the OTA is fixed at 100μA and the power supplies are given as V_{DD} and V_{SS}= 1.65 V.

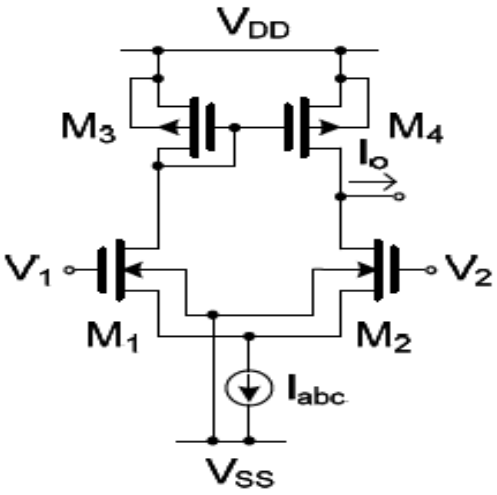

Fig.2.2. CMOS implementation of OTA

The OTA circuit in Fig.2.2 is simulated with Voltage V_1 sweeping from -1V to 1V with V_2 equal to 0V.

2.2.1. DC RESPONSE

The DC characteristics in Fig.2.3 shows a linear relationship between output current and input differential voltage $(V_1 - V_2)$ for -0.5V to +0.5V and having transconductance of 232.6mS.

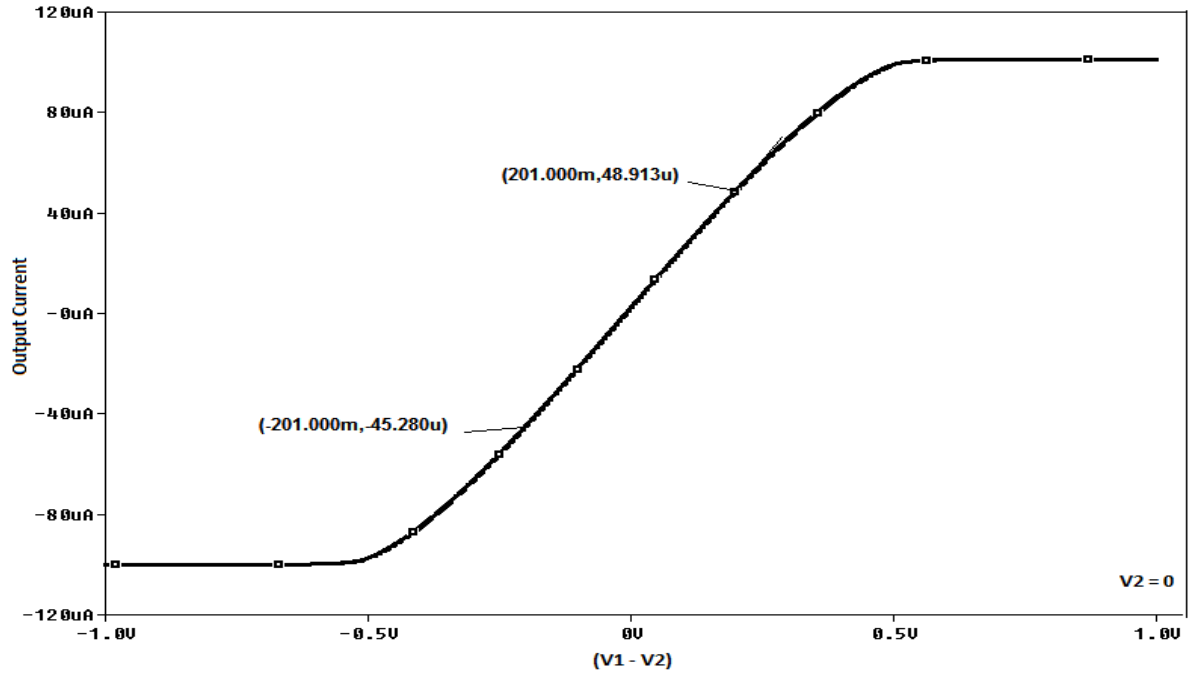

Fig.2.3. DC characteristics of OTA

The DC characteristics in Fig.2.4 shows a linear relationship between output current and input differential voltage ($V_1 - V_2$) for -0.5V to 0.5V for the three different curves (V_2= -0.25V, V_2 = 0V, V_2 = 0.25V) and all three having transconductance of 232.6mS.

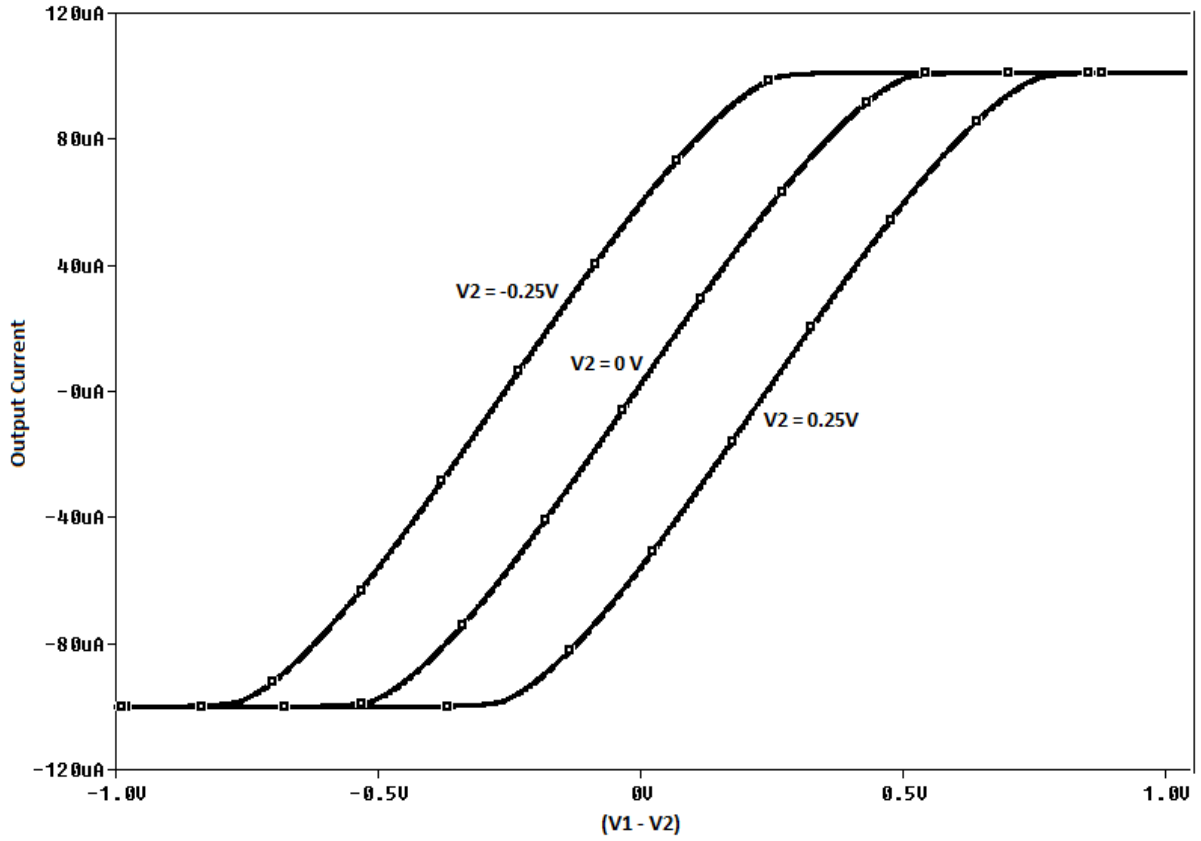

Fig.2.4. DC characteristics of OTA for three different value of V_2

2.2.2. AC RESPONSE

The AC characteristic shown in Fig.2.5 shows that OTA work well up to frequency of 80MHz because there is no roll off due to internal capacitances up to 80MHz.

The input condition for the AC response is given as V_2 is grounded and V_1 is provided with an AC source of 0.5V with its frequency sweeping from 300 KHz to 3GHz.

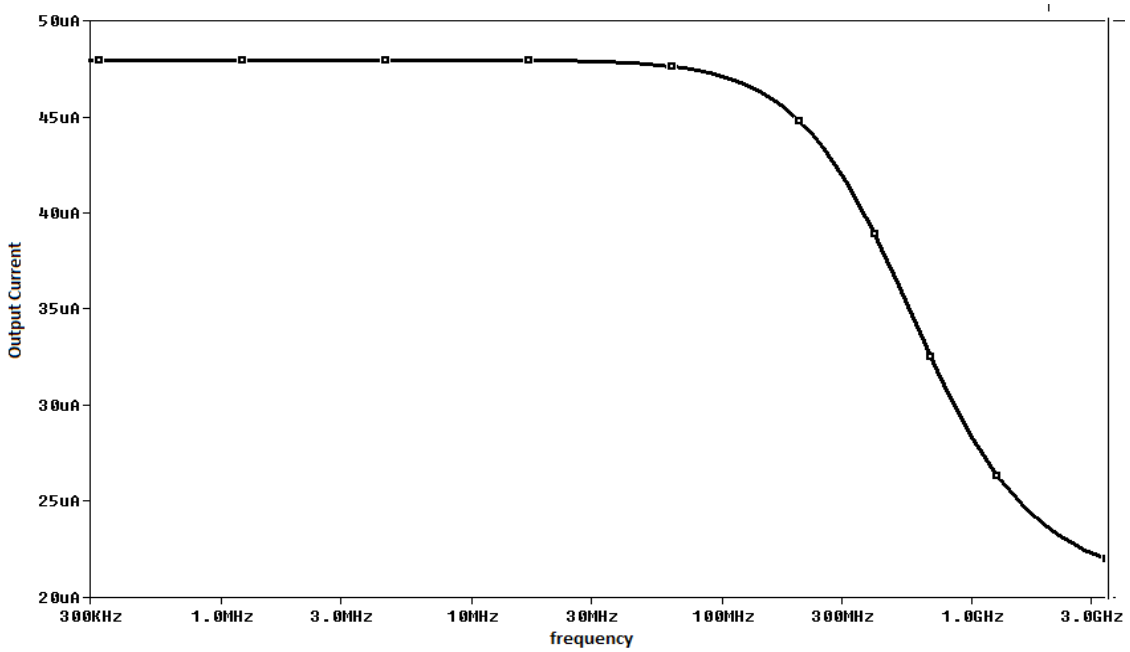

Fig.2.5. AC characteristics of OTA

2.2.3. TRANSIENT RESPONSE

The input condition for the transient response of Fig 2.6 is given as V_2 is grounded and V_1 is provided with an Sinusoidal source of 0.2 V amplitude with its frequency 1KHz and simulated for time 0 ms to 5 ms. The input condition for the transient response of Fig 2.7 is given as V_1 is grounded and V_2 is provided with an Sinusoidal source of 0.2 V amplitude with its frequency 1KHz and simulated for time 0 ms to 5 ms.

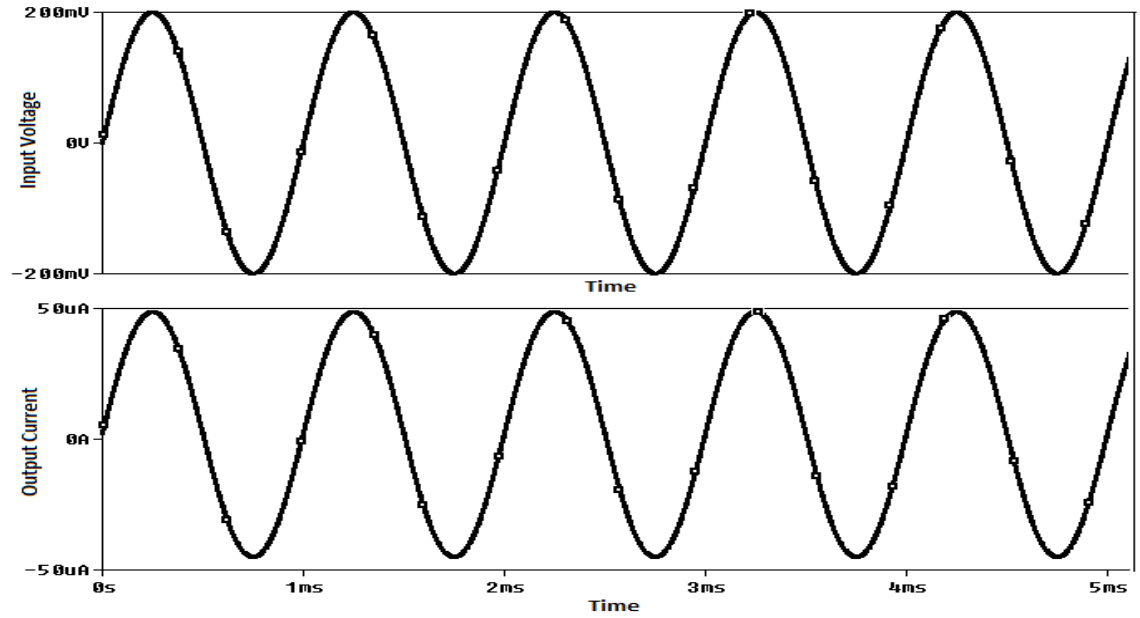

Fig.2.6. Transient response of OTA with input at V_1

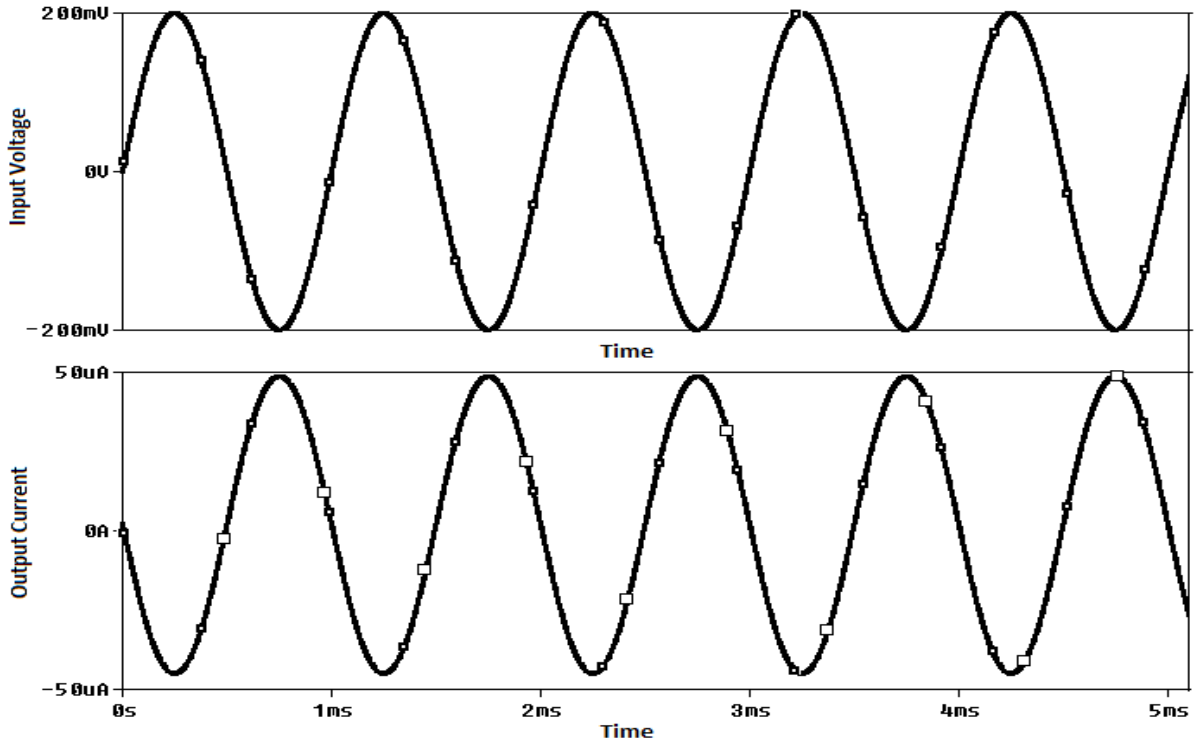

Fig.2.7. Transient response of OTA with input at V_2

2.3. SUMMARY

This Chapter presents "brief introduction of OTA and it is also studied and simulated. It is also characterized for DC, AC and transient responses and various performance parameters are extracted through SPICE simulations.

CHAPTER 3

OTA BASED APPLICATIONS

In this Chapter some basic circuit applications of OTA such as integrator, differentiator, divider, multiplier and MISO Universal filter are studied. The workings of these circuits have been validated through SPICE simulation. The theoretical and the observed results are found to be in close agreement hence verifying the functionality of OTA based applications.

3.1. DIFFERENTIATOR

3.1.1. CIRCUIT REALIAZATION

A differentiator is a circuit whose output is directly proportional to the rate of change of its input with respect to time. Differentiator generates square waveform for the triangular input waveform and for the input sine wave it produces cosine wave as an output. It is generally used in wave shaping circuits for detecting the high frequency component in any input signal. Differentiators are very important part in electronic analog computers and analog PI controllers. They are also used in frequency modulators as rate-of-change detectors.

Figure 3.1 shows the OTA-based differentiator. The equations of Fig. 3.1 are given below

$$I_1 = g_{m_1} v_{in}(t), \quad I_2 = -g_{m_2} v_c, \qquad I_1 = -I_2 \tag{3.1}$$

From the above three equations

$$v_c = \frac{g_{m_1}}{g_{m_2}} v_{in}(t) \tag{3.2}$$

and $$I_3 = g_{m_3} v_{diff}(t), \; I_3 = C\frac{dv_c}{dt} \tag{3.3}$$

Where I_1, I_2 and I_3 are output currents of OTA_1, OTA_2 and OTA_3 respectively. V_c is the voltage across capacitor. No current will flow into the input terminals of either OTA because all having very high input impedances. Combining all these equation we get (3.4). Which is the equation of the differentiator

$$v_{diff}(t) = \frac{g_{m1}c_1}{g_{m2}g_{m3}}\frac{d}{dt}[v_{in}(t)] = k_{dif}.\frac{d}{dt}[v_{in}(t)] \tag{3.4}$$

Where $v_{in}(t)$ is input applied to the OTA_1 and $k_{dif} = \frac{g_{m1}c_1}{g_{m2}g_{m3}}$ is the differentiator coefficient and gm_1, gm_2 and gm_3 denotes the transconductance of an OTA_1, OTA_2 and OTA_3 respectively.

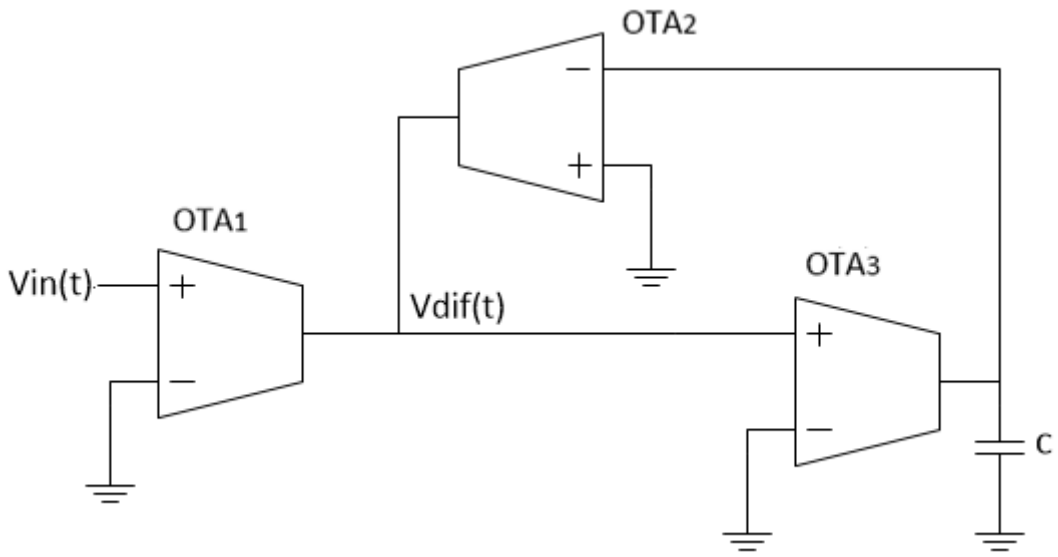

2.1 Fig3.1 OTA based differentiator

3.1.2.SIMULATION RESULTS

The differentiator circuit of Fig.3.1 using three OTAs is simulated using 0.35µm technology. The aspect ratio of transistors in all OTAs of Fig.3.1 are W/L=10µm/1µm for PMOS devices and W/L=5µm/1µm for NMOS devices. The circuit is simulated for two different functions, one is for ramp function shown in Fig.3.2 and other is for sinusoidal function in Fig.3.3 resulting in step function and cosine function"respectively. The "x axis in Fig.3.2 is the time axis taken from 0ms to 1ms and two graphs are plotted at y axis (with respect to time) one is ramp input and other is step output clearly showing that the output function is the differentiation of the input function.

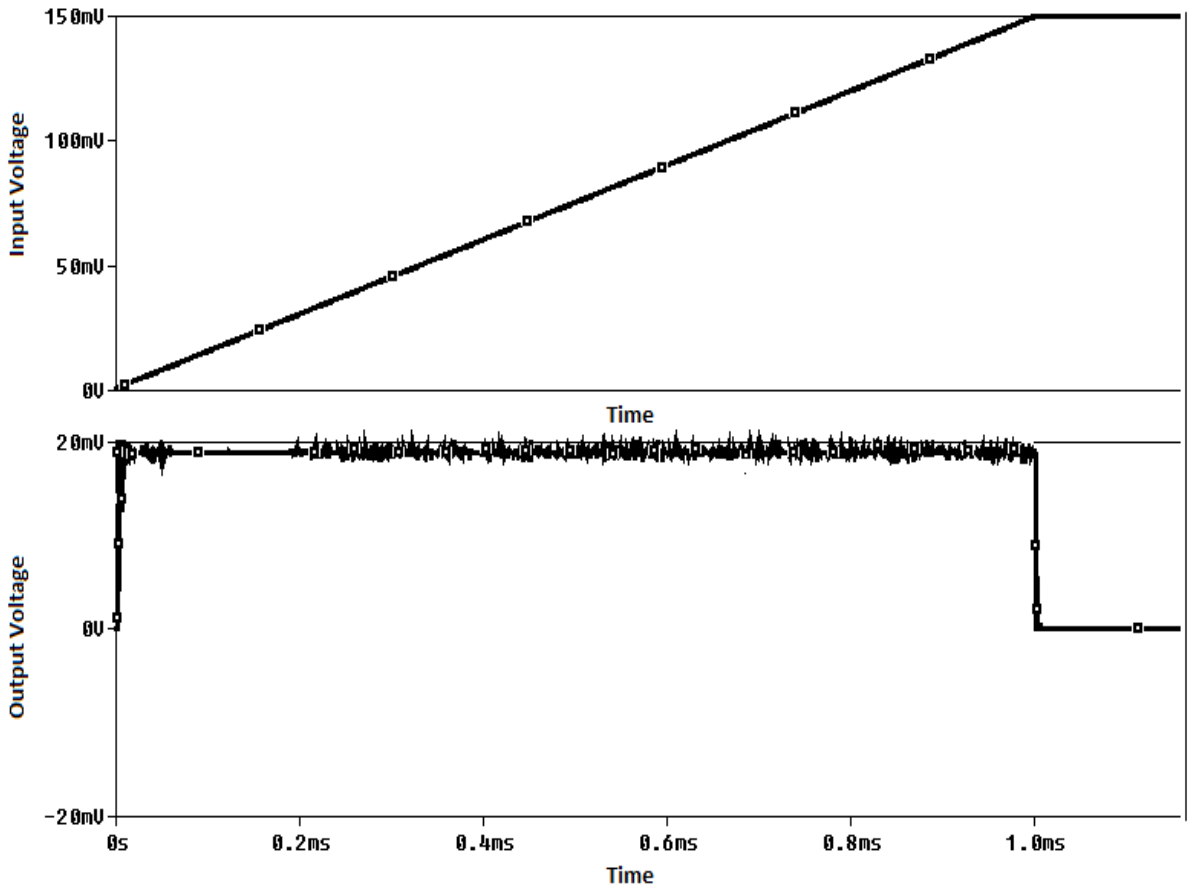

Fig.3.2. Step output for ramp input of OTA based differentiator

The x axis in Fig.3.4 is the time axis taken from 0ms to 5ms and two graphs are plotted at y axis (with respect to time) one is sine input and other is cosine output clearly showing that the output function is the differentiation of the input function.

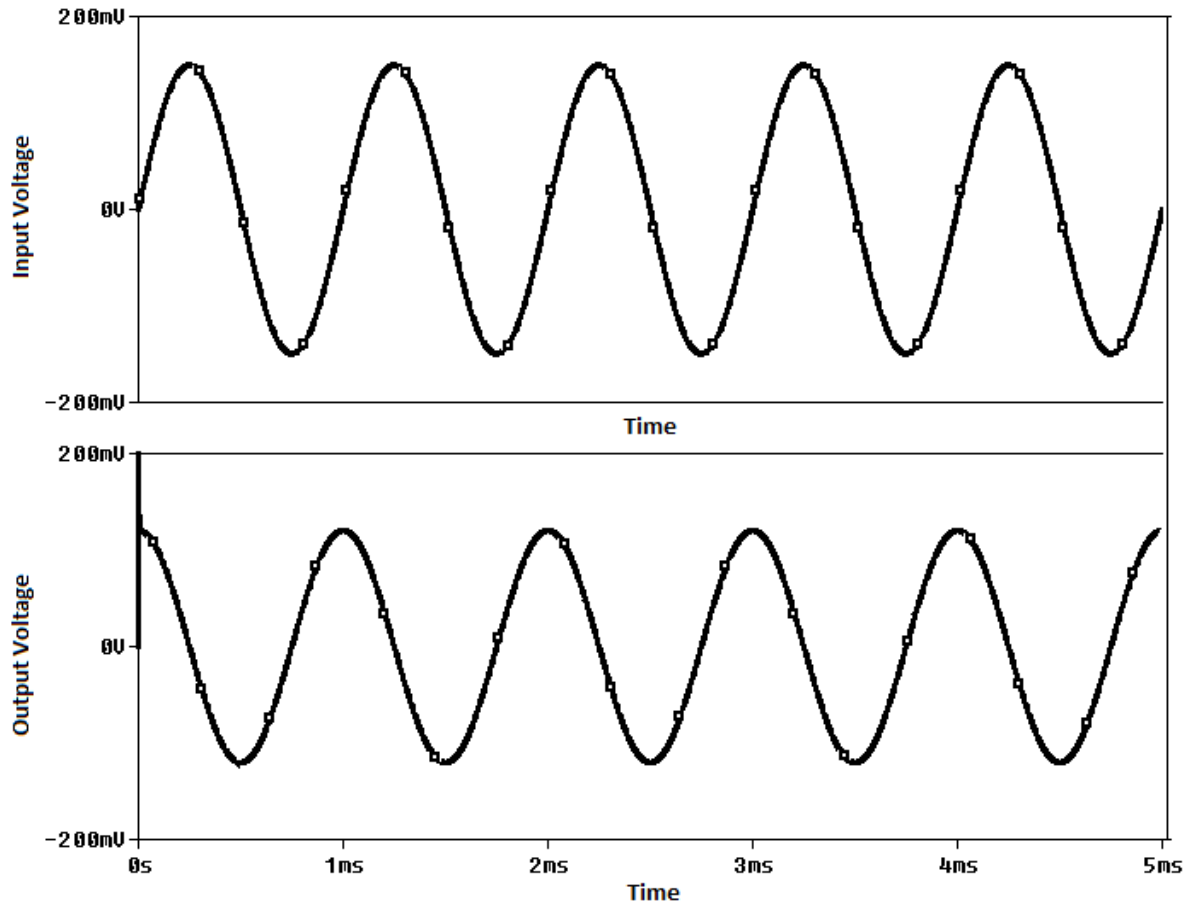

Fig.3.3. Cosine output for Sine input of OTA based differentiator

3.2. INTEGRATOR

3.2.1 CIRCUIT REALIAZATION

An integrator is a circuit whose output signal is directly proportional to the time integral of its input signal. Integrator acts as a low pass filter and generates sawtooth waveform for the square input waveform. Integrators are generally used in analogue-to-digital converters, ramp generators and also wave shaping applications.

Figure 3.4 shows the OTA-based integrator. Here $v_{in}(t)$ is applied to the inverting terminal of the operational transconductance amplifier.

From Fig. 3.4 the equation of output current I_o is given as

$$I_o = g_m v_{in}(t) \qquad (3.5)$$

$$I_o = C\frac{dv_{out}(t)}{dt} \qquad (3.6)$$

Combining the (3.5) and (3.6) the output of the integrator using operational transconductance amplifier is expressed as

$$v_{out}(t) = \frac{g_m}{c}\int v_{in}(t)dt = k_{int}\int v_{in}(t)\,dt \qquad (3.7)$$

Where $k_{int} = \frac{g_m}{c}$ is the integrator coefficient.

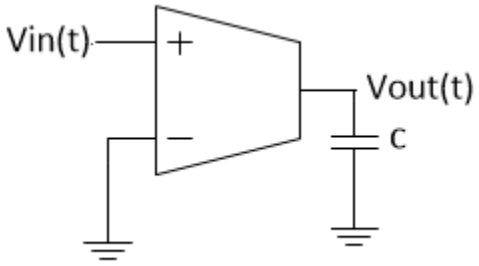

Fig.3.4 OTA based integrator

3.2.2. SIMULATION RESULTS

The integrator circuit of Fig.3.4 using single OTA is simulated using 0.35µm technology. The circuit is simulated for sinusoidal function in Fig.3.5 resulting in cosine function

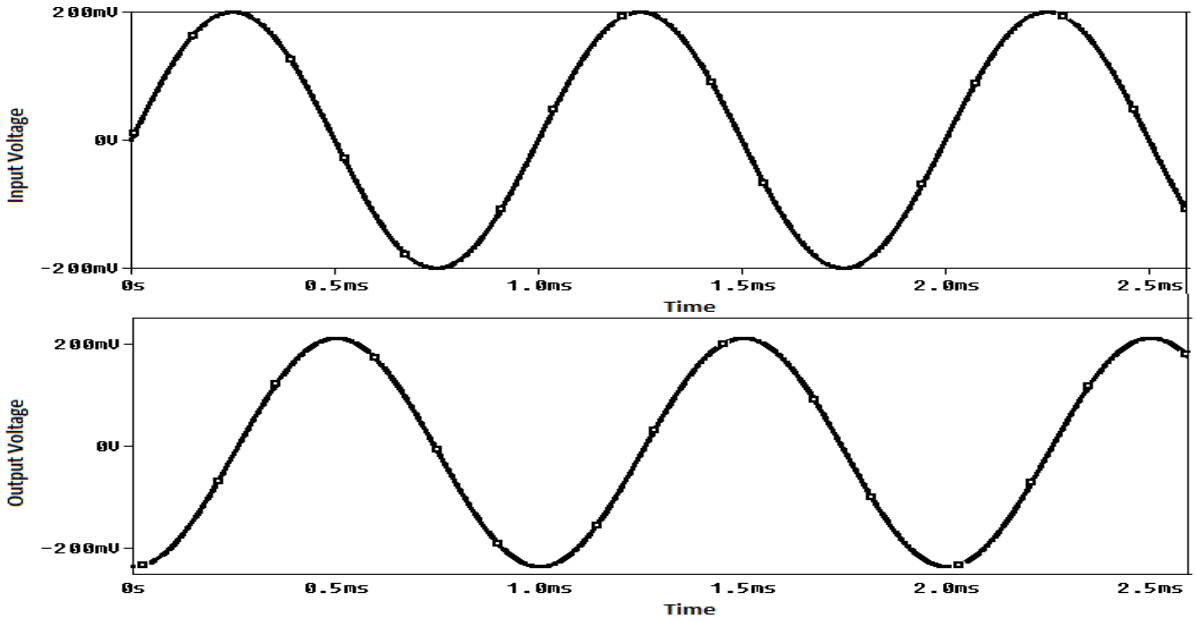

Fig.3.5. Cosine output for Sine input of OTA based Integrator

3.3. MULTIPLIER

3.3.1. CIRCUIT REALIZATION

Multiplier is an important nonlinear building block that is useful in wide range of applications such as telecommunication, control, instrumentation and signal processing. Recently the OTA has emerged as an alternate analog building block with linear input output characteristics. OTA provides an electronic tuning capability of its transconductance gain by adjusting its bias current or voltage and can be implemented by using both bipolar and CMOS technologies. Moreover, OTA-based circuits require no resistor which is idea .for integrated circuit implementation. The circuit of OTA based multiplier is shown in Fig.3.6. The inputs $v_{in1}(t)$ and $v_{in2}(t)$are applied to the OTA 1 and OTA2 respectively and v_{o_1} is the output of OTA1. The equations of Fig. 3.6 are given below

$$v_{o_1} = -R\, g_{m_1} v_{in_1}(t) \tag{3.8}$$

$$I = -R\, g_{m_1} g_{m_4} v_{in_1} \tag{3.9}$$

$$g_{m_1}\, \alpha\, \sqrt{I_{bias_1}}$$

$$g_{m_4}\, \alpha\, \sqrt{I_{bias_4}}$$

$$I_{bias_1} = g_{m_2} v_{in_2}(t) \tag{3.10}$$

$$I_{bias_4} = g_3 v_{in_2}(t) \tag{3.11}$$

$$I = -R\, \sqrt{g_{m_2} g_{m_3}}\, v_{in_1}(t).\, v_{in_2}(t) \tag{3.12}$$

The output of the multiplier is taken from OTA4 and is expressed as

$$I = -v_{in1}(t) v_{in2}(t) k_{mul} \tag{3.13}$$

Where k_{mul} is multiplier coefficient.

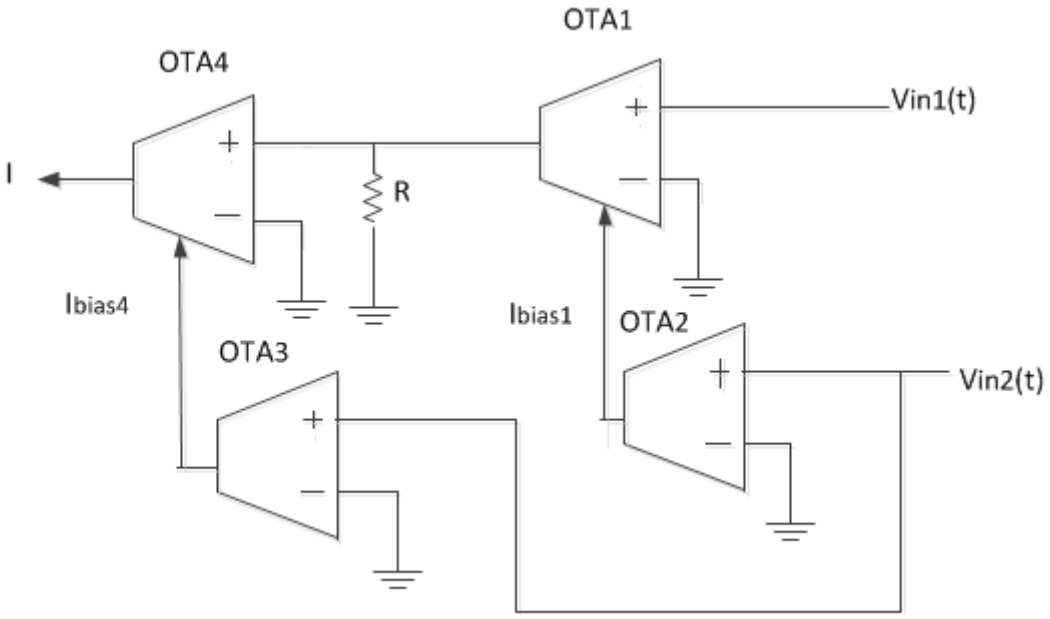

Fig.3.6. OTA based multiplier circuit

4.3.2. SIMULATION RESULTS

The OTA based multiplier circuit in Fig.3.6 consists of four OTAs and is simulated using 0.35µm technology. The aspect ratio of transistors in all OTAs of Fig.3.6 are W/L=10µm/1µm for PMOS devices and W/L=5µm/1µm for NMOS devices. The two voltages applied are v_1 and v_2 where v_1 is taken on x axis which sweeps from -100mv to +100mv and v_2 is taken as 0mv,-25mv and -50mv for which the output is taken on y axis. The dc characteristics of OTA based multiplier is shown in Fig.3.7.

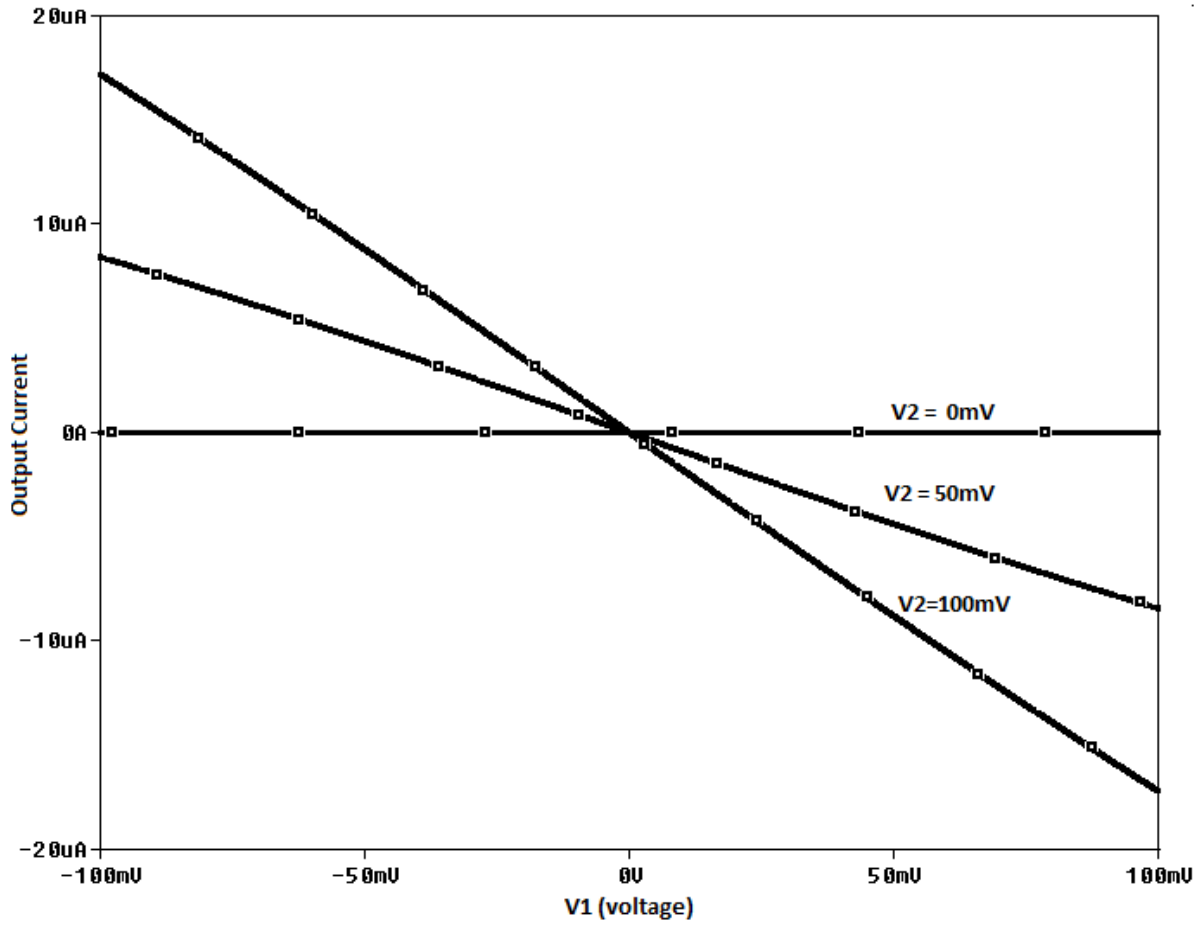

Fig.3.7. DC characteristics of OTA based multiplier

3.4. DIVIDER

3.4.1 CIRCUIT REALIZATION

Divider is an important nonlinear building block that is useful in wide range .of applications such as telecommunication, control, instrumentation and signal processing. Fig. 3.8 shows the OTA-based divider. The output of the divider is expressed as

$$v_{div}(t) = \left[\frac{v_{in1}(t)}{v_{in2}(t)}\right].K_{div} \qquad (3.14)$$

Where K_{div} is the divider coefficient.

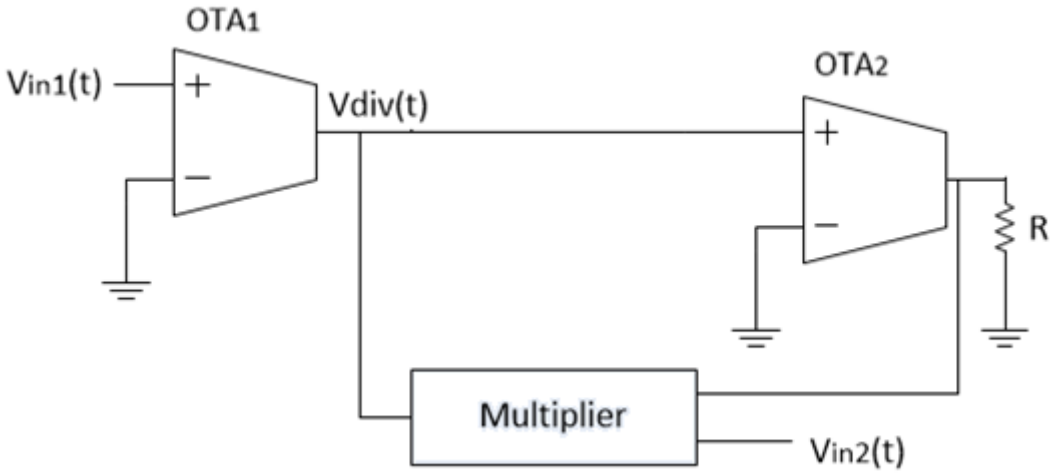

Fig.3.8 OTA based divider

3.4.1 SIMULATION RESULTS

The divider circuit is implemented using two OTAs and a multiplier of Fig.3.6 that is the integral part of the divider circuit. The divider circuit of Fig.3.8 is simulated using 0.35µm technology. The Fig 3.9 shows the divider function as $\frac{V_1}{V_2}$ where V_2sweeps from 0 to 100mv and V_1 is taken as -50mv 0mv and 50mv.

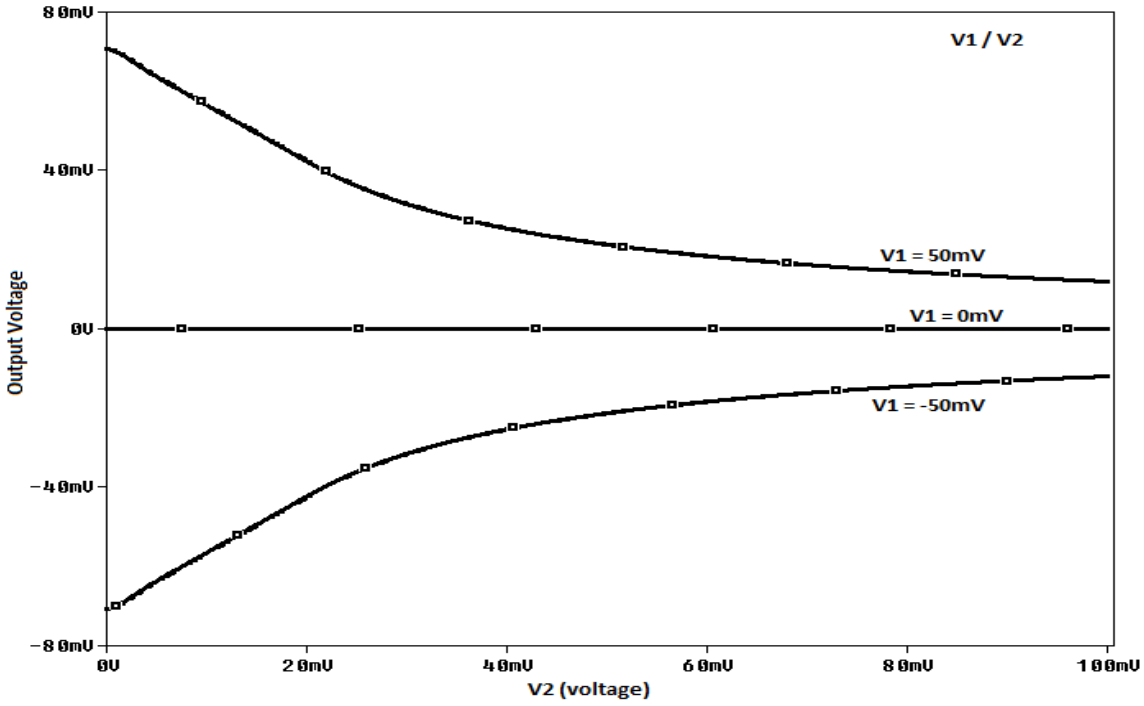

Fig.3.9. Divider output showing V1/V2 (V2: 0 to 100mv for V1: -50mv,0mv, 50mv)

3.5. MULTI INPUT SINGLE OUTPUT UNIVERSAL FILTER

3.5.1 CIRCUIT REALIZATION

Depending on the number of the inputs provided and output obtained on the terminals, filters are classified into two classes: (i) single-input multiple-output (SIMO) [37]-[41] and (ii) multiple-input single-output (MISO) [37]-[48].The MISO filters provide variety of circuit characteristics with different input connections. In comparison with the SIMO filters, the MISO filters can result in reducing the number of active elements used and to realize a large variety of filter functions. MISO Universal filter provides low pass, band-pass, high-pass, band-stop and all pass filters in a single topology. Figure 3.10 represents a three-input one-output voltage mode electronically tunable voltage-mode universal biquadratic filter with three inputs and one output using five simple OTAs, two grounded capacitors and one MOS resistor[36]. The natural frequency and the quality factor of this filter can be controlled orthogonally and electronically by adjusting the bias currents. If v_{in1}, v_{in2} and v_{in3} are the input signal voltages, the output voltage v_{out} of Fig.3.10 can be expressed as

$$V_o = \frac{(s^2 C_1 C_2 R_1 + R_1 g_{m1} g_{m2})V_{in1} - (sC_2 R_1 g_{m3})V_{in2} - (R_1 g_{m1} g_{m2})V_{in3}}{s^2 C_1 C_2 + sC_1 R_1 g_{m2} g_{m3} + g_{m1} g_{m2}} \qquad (3.15)$$

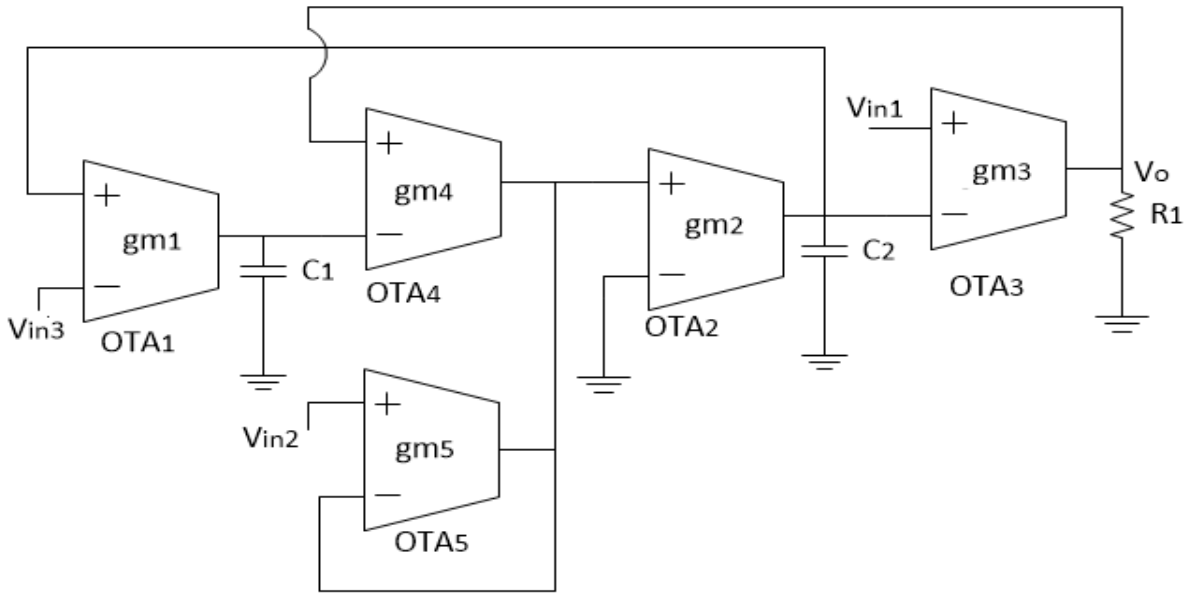

Fig.3.10. MISO Universal filter

From the Fig.3.10 low pass, high pass, band pass and band stop filters can be obtained as

Low pass: $V_{in1} = V_{sig,} V_{in2} = V_{in3} = 0$ (3.16)

Band pass: $V_{in2} = V_{sig,} V_{in1} = V_{in3} = 0$ (3.17)

Band stop: $V_{in3} = V_{sig,} V_{in1} = V_{in2} = 0$ (3.18)

High pass: $V_{in1} = V_{in3} = V_{sig,} V_{in2} = 0$ (3.19)

The natural frequency (ωo) and the quality factor (Q) of this MISO filter can be expressed as

$$\omega_o = \sqrt{\frac{g_{m1} g_{m2}}{C_1 C_2}} \quad (3.20)$$

$$Q = \frac{1}{R_1 g_{m3}} \sqrt{\frac{C_2 g_{m1}}{C_1 g_{m2}}} \quad (3.21)$$

3.5.2. SIMULATION RESULTS

The four configurations Low pass, Band pass, Band stop and High pass are implemented and simulated using 0.35µm CMOS technology by feeding the three inputs as explained in (3.6) to (3.9).The aspect ratio of transistors in all OTAs of Fig.3.10 are W/L=10µm/1µm for PMOS devices and W/L=5µm/1µm for NMOS devices. The biasing currents for OTA_4 and OTA_5 are fixed as 20µA and the power supplies are given as V_{DD} and V_{SS}= 1.65 V. Capacitor C_1 and C_2 are of 10pF and the biasing currents I_{abc1}= I_{abc2}= 50µA, I_{abc3}=37µA. The AC characteristics of all configurations are plotted using frequency log axis from 30 KHz to 30 MHz showing Low pass, High pass, Band pass and Band stop filters.

In Fig.3.11 the x-axis is the frequency axis where frequency is taken from 30 KHz to 30 MHz on log scale. The plots indicate the gain at y-axis of a low pass filter.

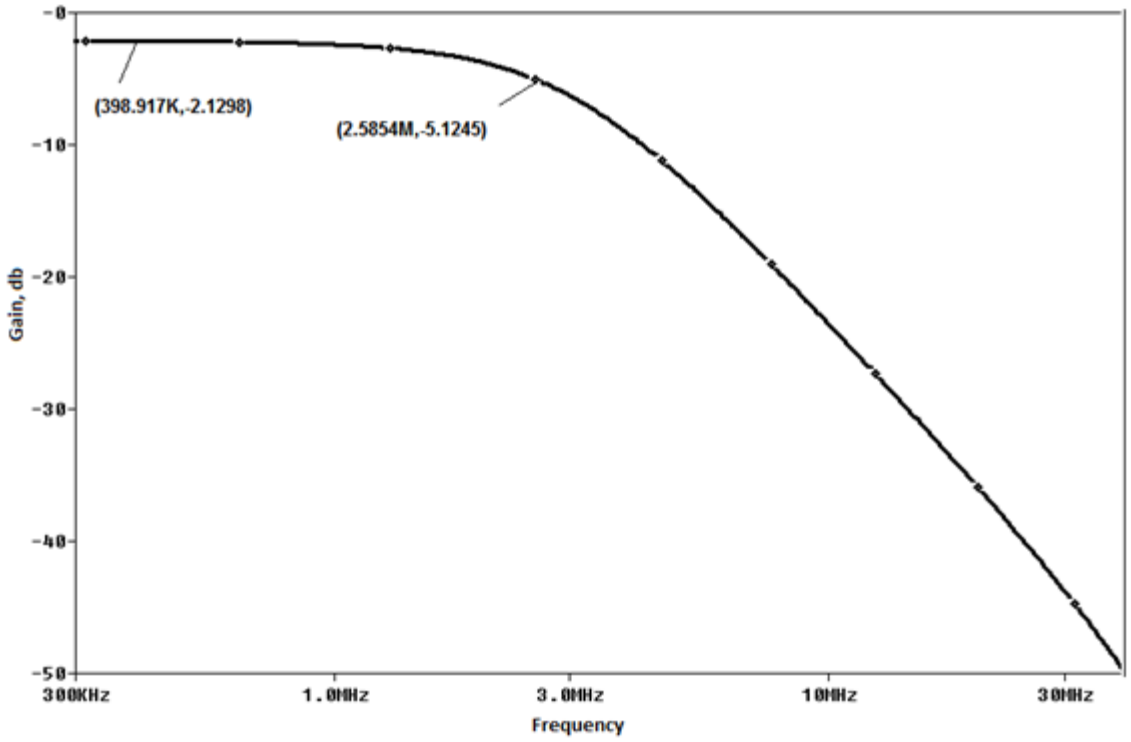

Fig.3.11. Frequency response of low pass filter configuration

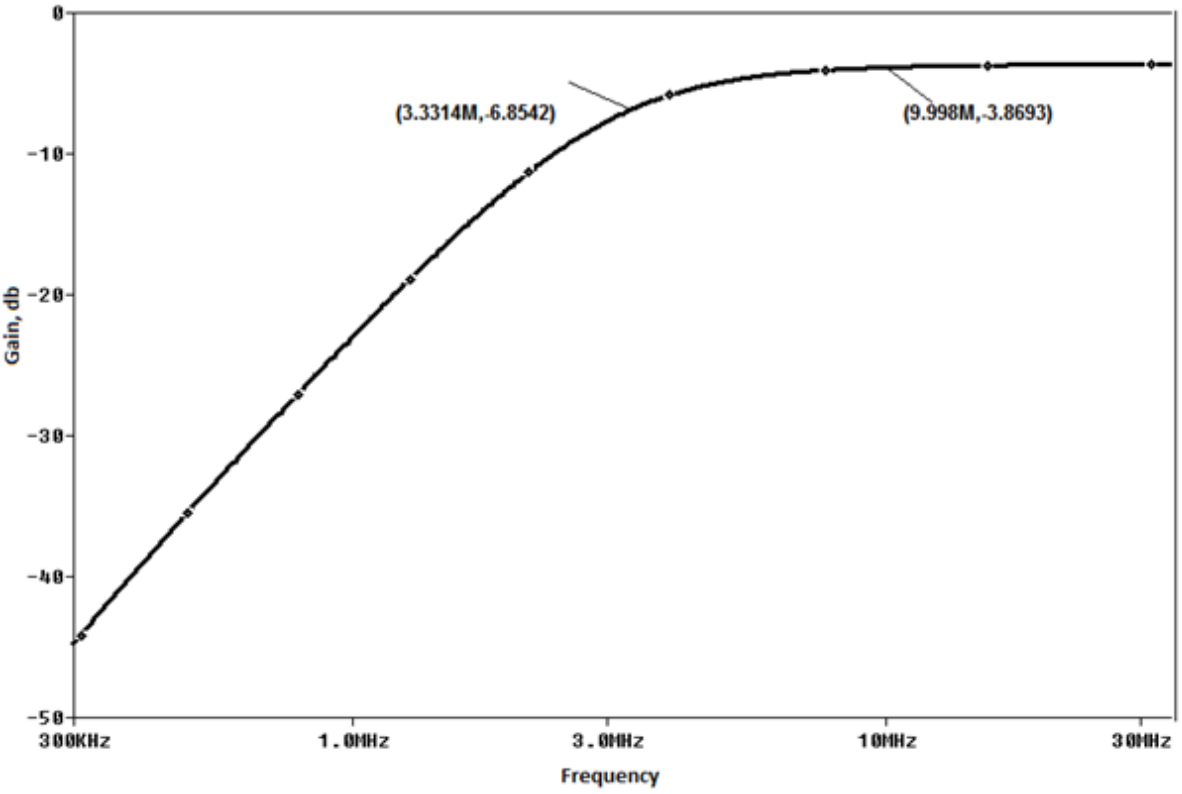

Fig.3.12. Frequency response of high pass filter configuration

In Fig.3.12 the x-axis is the frequency axis where frequency is taken from 30 KHz to 30 MHz on log scale. The plots indicate the gain at y-axis of a high pass filter.

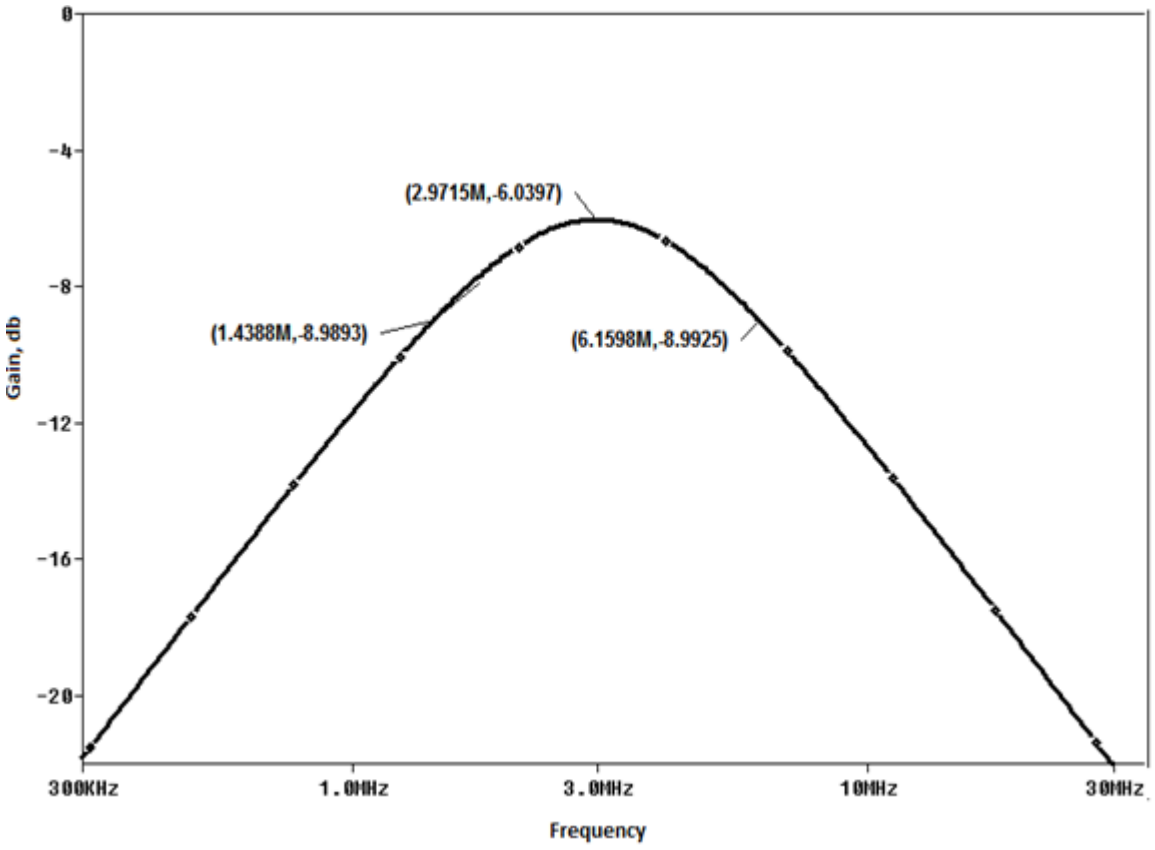

Fig.3.13. Frequency response of band pass filter configuration

In Fig.3.13 the x-axis is the frequency axis where frequency is taken from 30 KHz to 30 MHz on log scale. The plots indicate the gain at y-axis of a band pass filter.

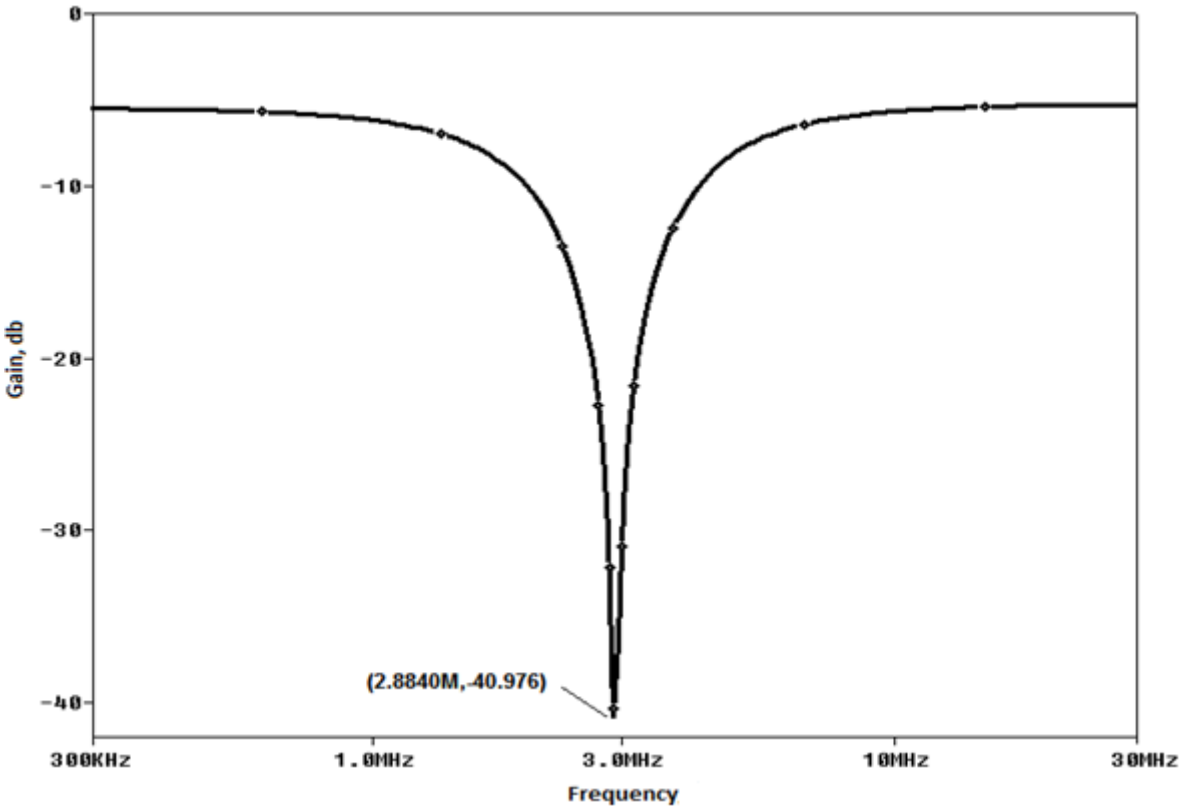

Fig.3.14. Frequency response of band stop filter configuration

The x-axis is the frequency axis where frequency is taken from 30 KHz to 30 MHz on log scale. The plots indicate the gain at y-axis of a band stop filter.

3.6. SUMMARY

In this chapter some existing applications of OTA are implemented and verified through SPICE simulator. The applications include differentiator, integrator, divider, multiplier and multi-input single output voltage-mode Universal filter.

CHAPTER 4

LITERATURE SURVEY OF SHADOW FILTER

4.1. INTRODUCTION

The characteristics of a filter for example characteristic frequency, quality factor and bandwidth can be modified either by altering the values of the passive components that are utilized in designing the filter or by adjusting active block trans-conductance electronically

New method for electronic tuning of the filter parameters has been implemented in a recently proposed family of second-order filters [17] known as the shadow filters. Here an external amplifier is placed in the feedback path and its gain (G) is varied to change the filter characteristics. This concept is popularly known as shadow filter and is gaining research interest [17]-[27]. In these filters, the filter characteristics zero to infinity while in practice from very low to very high. This is because of its ability of modifying the various parameters of the filters; for example the bandwidth, over a wide range by only adjusting the gain using amplifier. A fast hop between the two continuous center frequencies may be achieved. The theory of shadow filter can be applied to voltage- mode or the current-mode circuits.

Various terminologies have been used to realize the shadow filters in the past. In this chapter the terminologies related to shadow filter are reviewed.

4.2. AVAILABLE TOPOLOGIES OF SHADOW FILTER

The generalized block diagram of second order shadow filter is shown in Fig.4.1 [28] in which inputs and outputs are in the form of voltage. So it is called to be working in voltage mode. H(s) is a band-pass transfer function while $H_1(s)$ is a low-pass transfer function, both being of second order with the same denominator and the characteristics of the modified transfer function H'(s) = Vo/Vin retains the band-pass characteristics but with constant centre frequency, variable Q, and constant value of the product of centre frequency and Q.

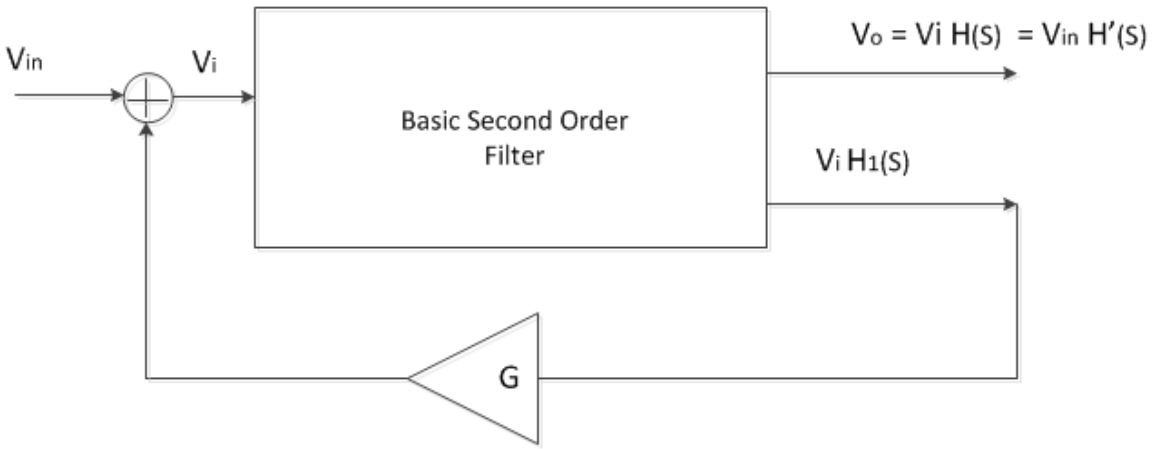

Fig.4.1. Second order voltage mode shadow filter

The feedback in the Fig.4.1 can be taken from any output s or a combination of them. Thus H(s) and H1(s) are of the forms.

$$H(s) = \frac{d+es+fs^2}{s^2+\left(\frac{\omega o}{Q}\right)+\omega o^2} \quad (4.1)$$

$$H_1(s) = \frac{a+bs+cs^2}{s^2+\left(\frac{\omega o}{Q}\right)+\omega o^2} \quad (4.2)$$

By analysis of Fig. 1, we get

$$H'(s) = \frac{H(s)}{1-GH_1(s)} \quad (4.3)$$

From (4.1), (4.2) and (4.3) we get

$$H'(s) = \frac{d'+e's+f's^2}{s^2+\left(\frac{\omega' o}{Q'}\right)s+\omega' o^2} \quad (4.4)$$

Where (d', e', f',) = $(d,e,f)/(1-Gc)$

$\omega o' = \sqrt{(\omega o^2 - Ga)/(1-Ac)}$; $Q' = \sqrt{(1-Gc)/\omega o^2 - Ga)}/(\omega o - GbQ)$

The topology of shadow filters in Fig.4.1 does not provide orthogonal tuning of filter characteristics. This limitation is overcome by placing two parallel amplifiers in feedback loop and thus providing orthogonal tuning which is shown in Fig.4.2. In this topology two

outputs at the same time are feedback to the input but it uses the summer amplifier in its circuit. In Fig 4.2 [15] the outputs V_{LP} and V_{BP} are feedback to the input.

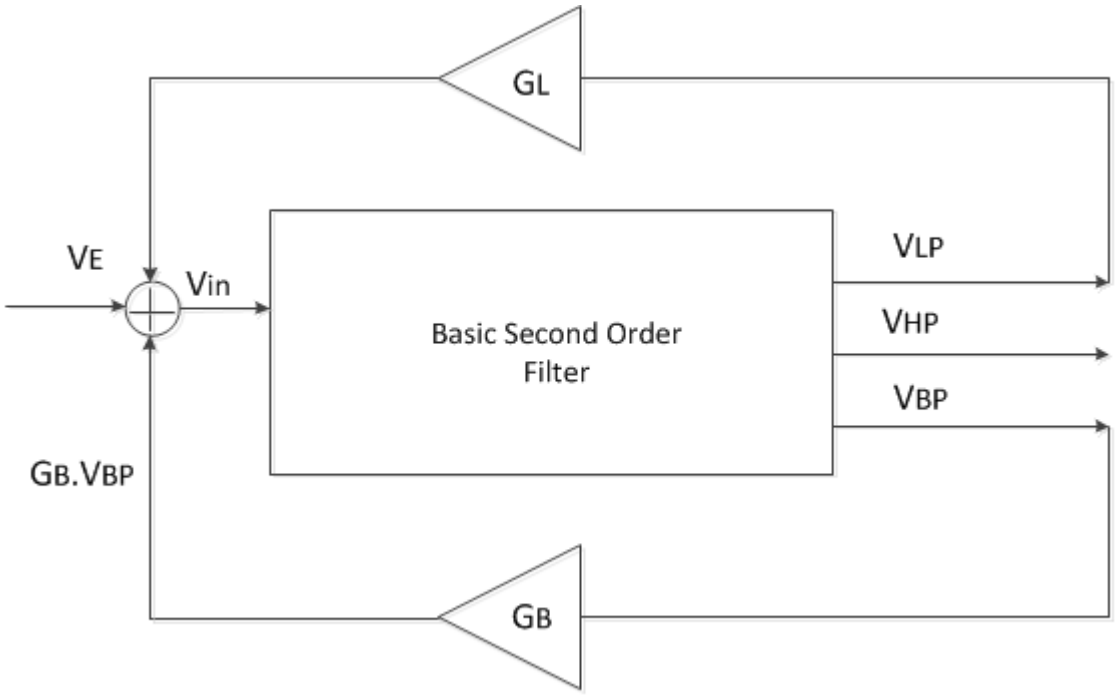

Fig.4.2.Voltage mode shadow filter with two feedback

Topologies shown in Fig.4.1 and Fig.4.2 uses additional summer amplifier in its circuit to overcome this drawback a new topology which eliminates the need of the summer in the shadow filter circuit is shown in Fig.4.3 which is in the form of multiple input single output [29]. Figure 4.3 shows the one feedback multiple input single output voltage mode shadow filter.

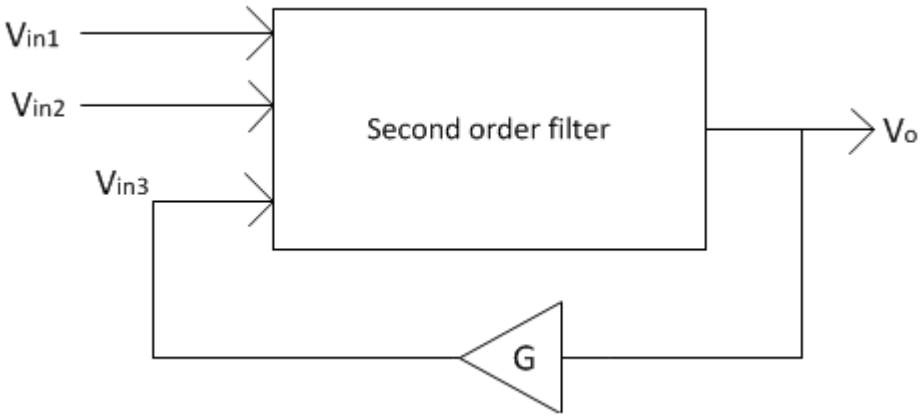

Fig.4.3.multi input single output one feedback shadow filter

Shadow filter topology shown in Fig.4.3 uses single feedback therefore a single parameter of shadow filter either frequency or bandwidth can be controlled at a time. A new topology in which both the center frequency and bandwidth can be controlled at the same time by using two feedback amplifiers with gain G1 and G2 [29] is shown in Fig.4.4.

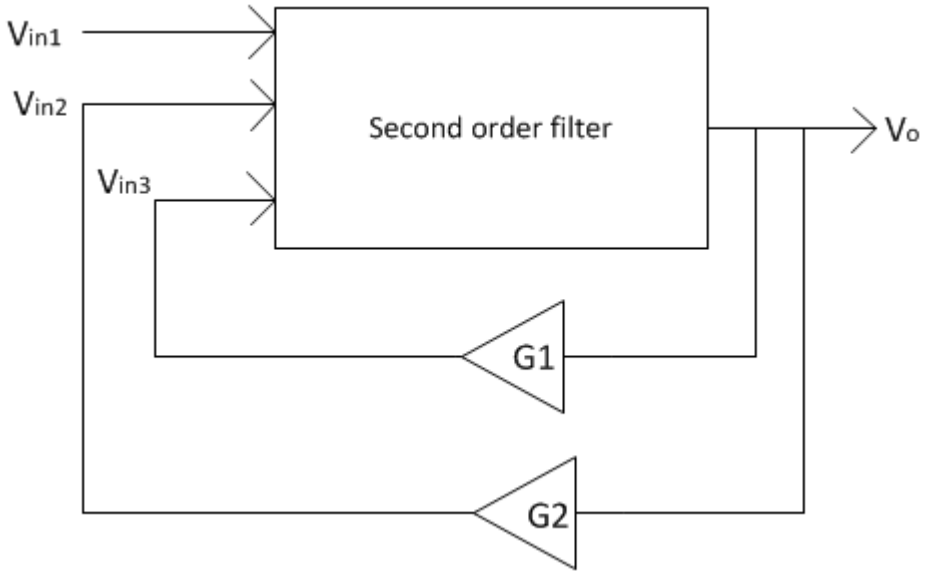

Fig.4.4. Multi input single output two feedback shadow filter

A topology shown in Fig.4.1 in which inputs and outputs are in the form of voltage but at new topology is also possible in which the inputs and outputs are in the form of current and is named as current mode second order shadow filter is shown in Fig.4.5.

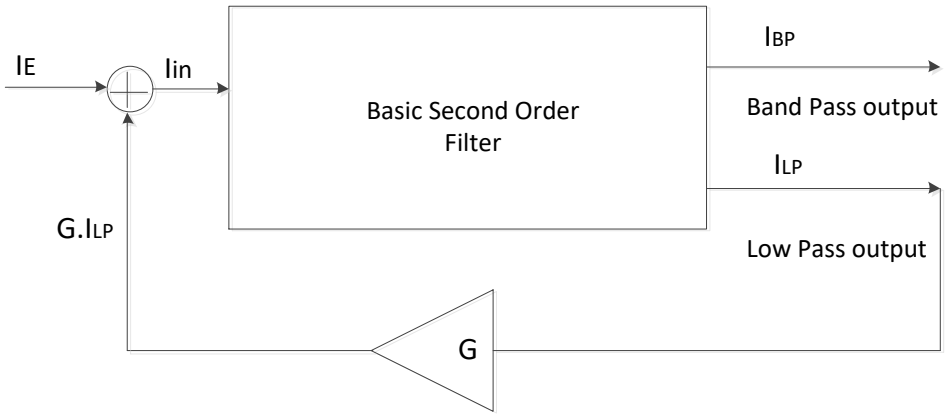

Fig.4.5. Second order current mode shadow filter

A topology shown in Fig.4.2 in which inputs and outputs are in the form of voltage and two outputs at the same time are feedback to the input. Relative to this topology at new topology is also possible in which the inputs and outputs are in the form of current and two outputs in the form of current at the same time are feedback to the input and is named as current mode second order shadow filter with two feedbacks is shown in Fig.4.6. In Fig 4.6 [18] the outputs I_{LP} and I_{BP} are feedback to the input.

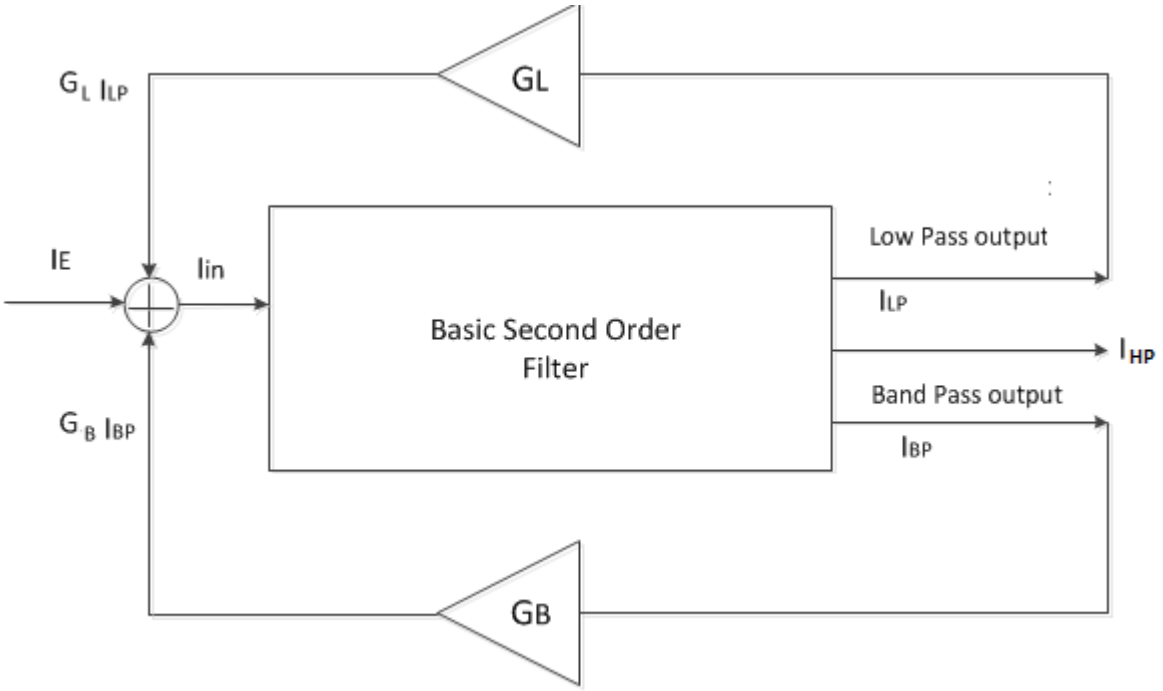

Fig.4.6. Second order current mode shadow filter with two feedback

4.3. CLASSIFICATION OF SHADOW FILTERS

Shadow filters are also classified as class-1, class n-1 and class n. In [19] the shadow filter generalization to nth class has been introduced in which shadow filters are extended to class n filters where n is positive integer. Figure 4.7 shows the Class n-1 shadow filter, the low pass output of which is amplified by a factor (1 - G) in order to get the gain back to its initial value (unity). Fig.4.8 shows the class n shadow filter its centre frequency is given by $f_0 G_n = f_0 G_n (n-1)\sqrt{(1-G)} = f_0 \mathrm{G}(1-G)^{0.5}$

In class n shadow filter the gain of the band pass output remains unchanged while the gain of the low pass output is divided by (1 - G).

Fig.4.7.Class n-1 shadow filter

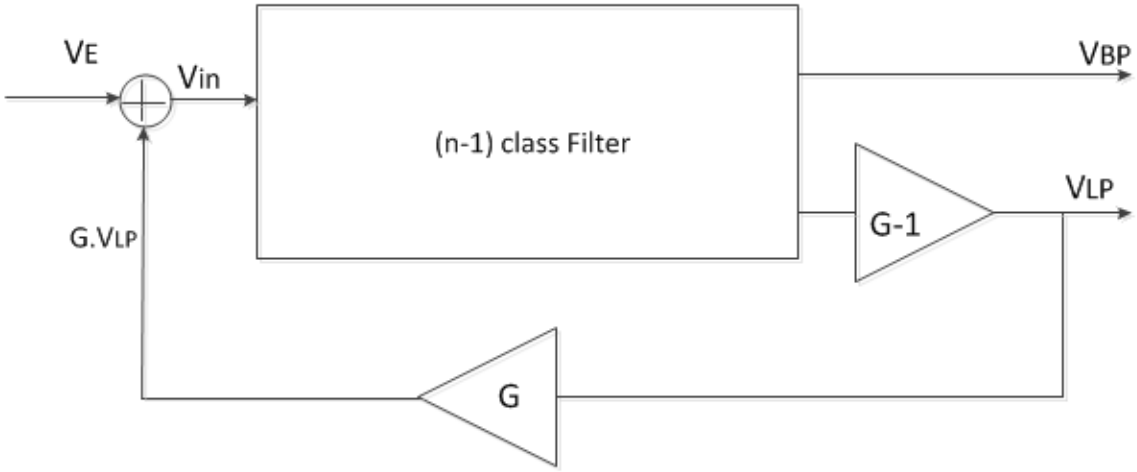

Fig.4.8.Class n shadow filter

4.4. AVAILABLE LITERATURE

Available literature shows that various active blocks have been used for the implementation of shadow filters. In [17] the implementation of second generation current controlled conveyor (CCCII) based current-mode shadow filter has been presented. The circuits have utilized four CCCII blocks and are used for realizing a band pass filter having variable center frequency and quality factor but keeping the bandwidth constant. The CCCII has also been used in [27] to realize a band pass shadow filter. In [18] the idea of [17] has been extended

to control the bandwidth and the quality factor keeping the center frequency constant. In [18] a Z-copy of current inverter trans-conductance amplifier (ZCCITA) based current-mode band pass filter has been presented. The circuit has used the two ZC-CITA blocks and also two current amplifiers. The idea of [17] was extended in [19] in which a CCCII based shadow filter generalization to class-n. In [20] the idea of [1] was further extended to keep constant the center frequency and varying the quality factor but no practical implementation was shown in [20]. Practical applications of CCCII based shadow filters were proposed in [21–24]. Shadow filters utilizing the current difference transconductance amplifier (CDTA) and the voltage difference transconductance amplifier (VDTA) were proposed in [25] and [26] but these are not easily available ICs. In [29] new voltage-mode shadow filters have been presented and it has utilized easily available current-feedback operational-amplifier (CFOA). The circuits have been implemented in voltage mode, and not in the current-mode as presented in [17–19], [21–27]. In [30] a new shadow filter is presented using operational transresistance amplifier (OTRA). In which an amplifier is added externally in the feedback path of the filter and by controlling the gain of an amplifier the characteristics of this filter is tuned and depending on the value of gain of the external amplifier the filter characteristics are varied from low values to the high values. New Voltage mode shadow band pass filter is presented in [31] using current-feedback operational-amplifier (CFOA) and the parameters of the filter are controlled by varying the gain of external amplifier. In [32] new voltage-mode shadow filters using low-voltage low-power differential difference current conveyor (DDCC) has been realized. A new topology for realization of shadow band pass filter using the current-feedback operational amplifier (CFOA) has been presented in [33]. The proposed circuit has utilized the CFOAs, avoiding the external summing amplifier for implementing the shadow band pass filter with controlled center frequency. In [34] a new frequency agile filter has been presented with 3 dB bandwidth of 14 MHz for a wideband LNA, which provides 9.5 dB selectivity at 40 MHz frequency offset and the band gain is also reduced due to the switch on time of mixer switches. In [35] a new frequency agile filter for analog signal processing has been presented by using MOS only technique. As compared to the other building blocks, in analog this filter is realized using the MOS transistors only and the parasitic capacitances of the MOS transistors are used avoiding the use of the classical capacitors providing the advantages of improved frequency range and the low power consumption.

4.5. SUMMARY

In this chapter gives the brief introduction of shadow filter. Various available topologies of the shadow filter are discussed. The classification of shadow filter based on the class has also been provided, also an extensive survey of shadow filters has been provided.

CHAPTER 5

SINGLE FEEDBACK SHADOW FILTER

The shadow filters can have single feedback or two feedback structures. In this Chapter new structure of single-feedback shadow filter is proposed and the various configurations of single-feedback shadow filters like band pass shadow filter, high pass shadow filter, low pass filter and notch filter shadow filter are also implemented. The present work uses OTA as an active block for developing these shadow filters circuits.

5.1. PROPOSED OTA SHADOW FILTER USING SINGLE FEEDBACK

The block diagram of the proposed single feedback shadow filter structure is shown in Fig.5.1. The proposed shadow filter in Fig.5.1 does not require additional summing circuit in contrast to the shadow filter [17] as it is built with three inputs one output second-order filter [36] instead of one input two outputs second-order filter [17].

The second-order filter transfer function presented in [29] can be expressed as

$$Vo = \frac{T_1(s)V_{in1} - T_2(s)V_{in2} - T_3(s)V_{in3}}{a_2s^2 + a_1s + a_0} \qquad (5.1)$$

With $V_{in3} = GV_o$ where G is positive real number, then the transfer function of the structure of Fig.5.1 can be expressed as

$$V_o = \frac{T_1(s)V_{in1} - T_2(s)V_{in2}}{a_2s^2 + a_1s + a_0 + GT_3(s)} \qquad (5.2)$$

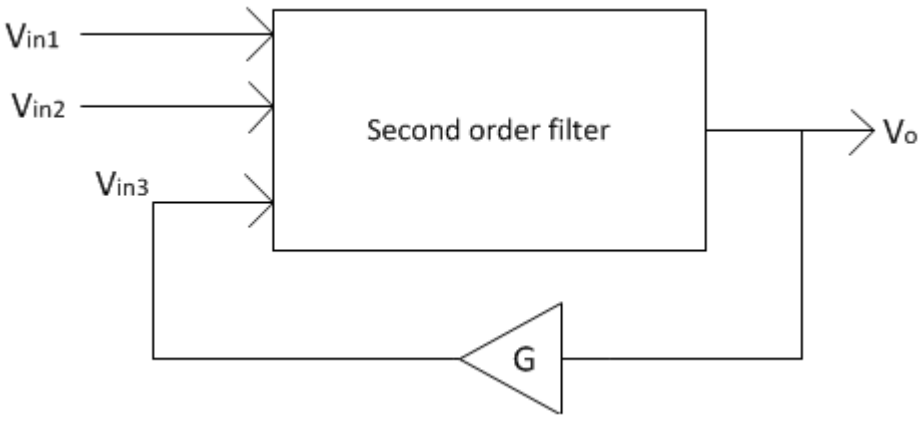

Fig.5.1 Single feedback shadow filter structure

5.2.PROPOSED BANDPASS SHADOW FILTER WITH CONTROLLABLE CENTER FREQUENCY

5.2.1. CIRCUIT REALIZATION

Figure 5.2 shows a proposed shadow band pass filter. It is obtained by modifying the topology given in [36]. In Fig.5.2 the external voltage amplifier with gain G is built around the circuit of Fig.3.10 from V_o to V_{in3} with input signal applied to V_{in2} and V_{in1} grounded.

The transfer function for Fig. 5.2 is computed as

$$V_o = \frac{\left(\frac{R_1}{C_1} g_{m3} s\right) V_{sig}}{s^2 + \frac{R_1 g_{m2} g_{m3}}{C_2} s + \frac{g_{m1} g_{m2}}{C_1 C_2} + G \frac{R_1 g_{m1} g_{m2}}{C_1 C_2}} \quad (5.3)$$

Where $G = g_{m6} R_2$

Equation (5.3) is the transfer function of a Band Pass filter with center frequency and Bandwidth given by

$$\omega_o = \sqrt{\frac{g_{m1} g_{m2}}{C_1 C_2} (1 + G R_1)} \quad (5.4)$$

$$BW = \frac{R_1 g_{m2} g_{m3}}{C_2} \quad (5.5)$$

Equation (5.4) shows that the center frequency of band pass filter can be controlled by the gain G of the external amplifier and the bandwidth remains constant.

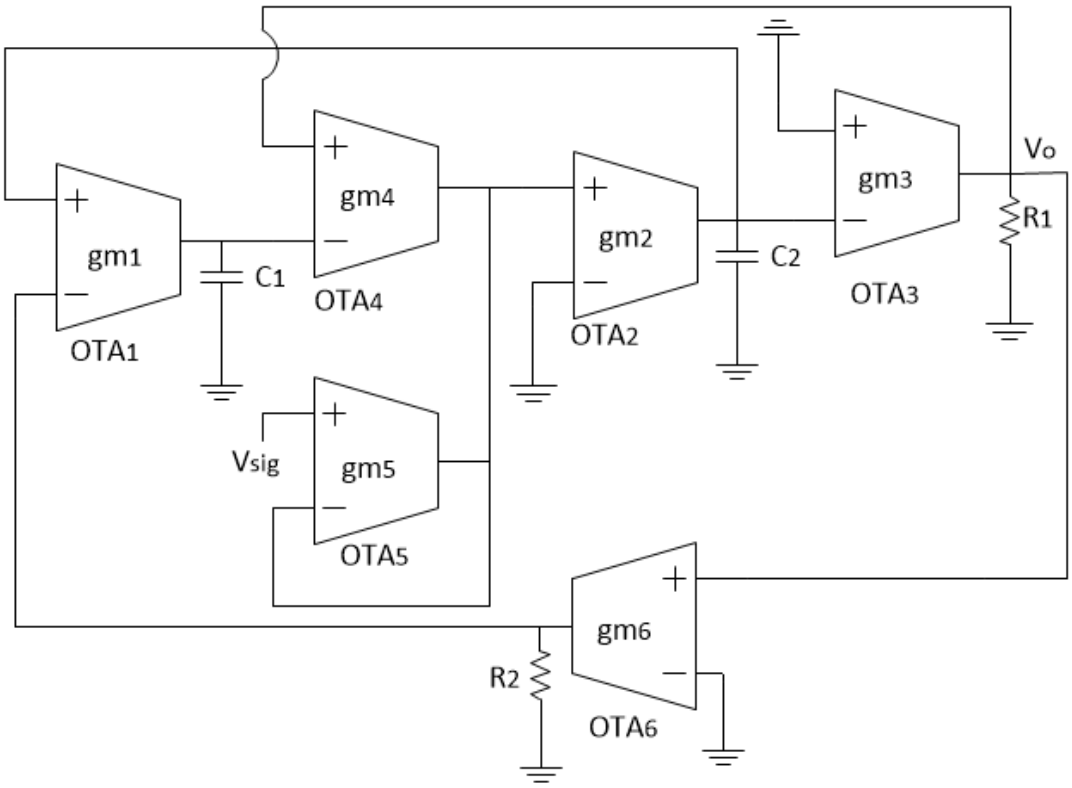

Fig.5.2. OTA- based voltage-mode shadow band pass filter

5.2.2.SIMULATION RESULTS

The SPICE schematics of OTA based voltage mode shadow band pass filter is shown in Fig.5.3.The shadow band pass filter is verified through SPICE simulators using the circuit of Fig.5.3 with 0.35 µm CMOS process from TSMC. The aspect ratio of transistors in all OTAs of Fig.5.3 are W/L=10µm/1µm for PMOS devices and W/L=5µm/1µm for NMOS devices. The power supplies are given as V_{DD}= -V_{SS}= 1.65 V. Capacitor C_1 and C_2 are of 10pF and the biasing currents I_{abc1}= I_{abc2}= 50µA, I_{abc3}=37µA.The biasing currents for OTA_4 and OTA_5 are fixed as 20µA. Other circuit components are taken as C_1 = C_2 = 10pF, R_1 = 10kΩ, R_2 = 5kΩ. Figure 5.4 shows simulated frequency response where the four traces represent four different values of gain (G, 2G, 4G, 8G). It can be clearly seen that the center frequency is varying with gain G of the feedback amplifier having value 3.6 MHz for gain G, 4.13 MHz for gain 2G, 4.88MHz for gain 4G and 5.8 MHz for gain 8G.

.

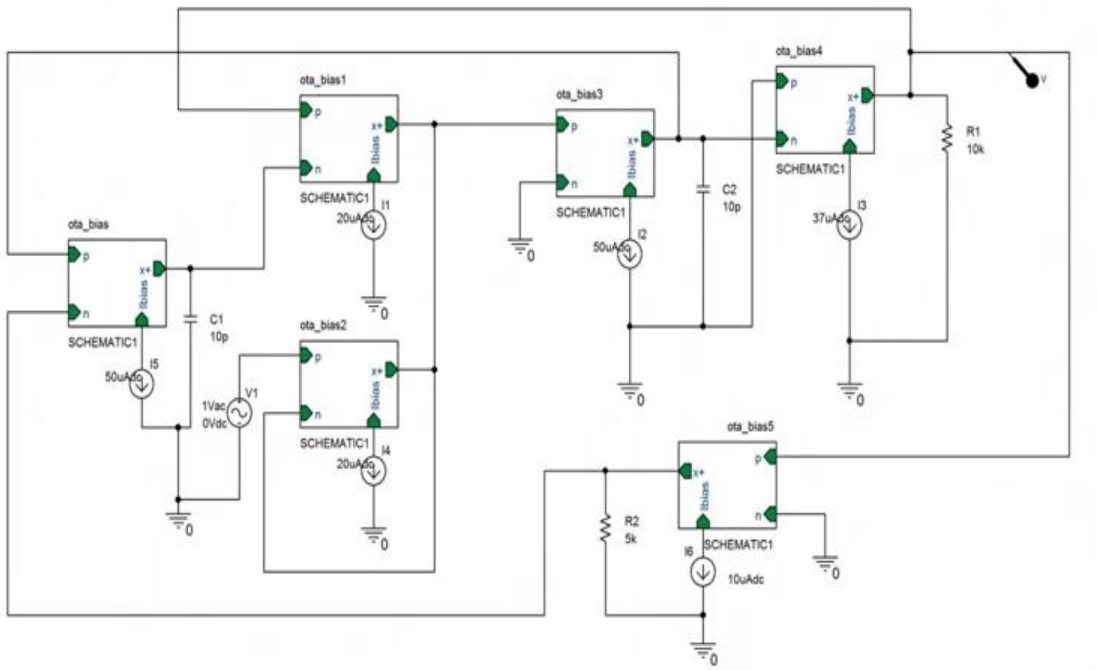

Fig.5.3. SPICE schematic of OTA based shadow band pass filter

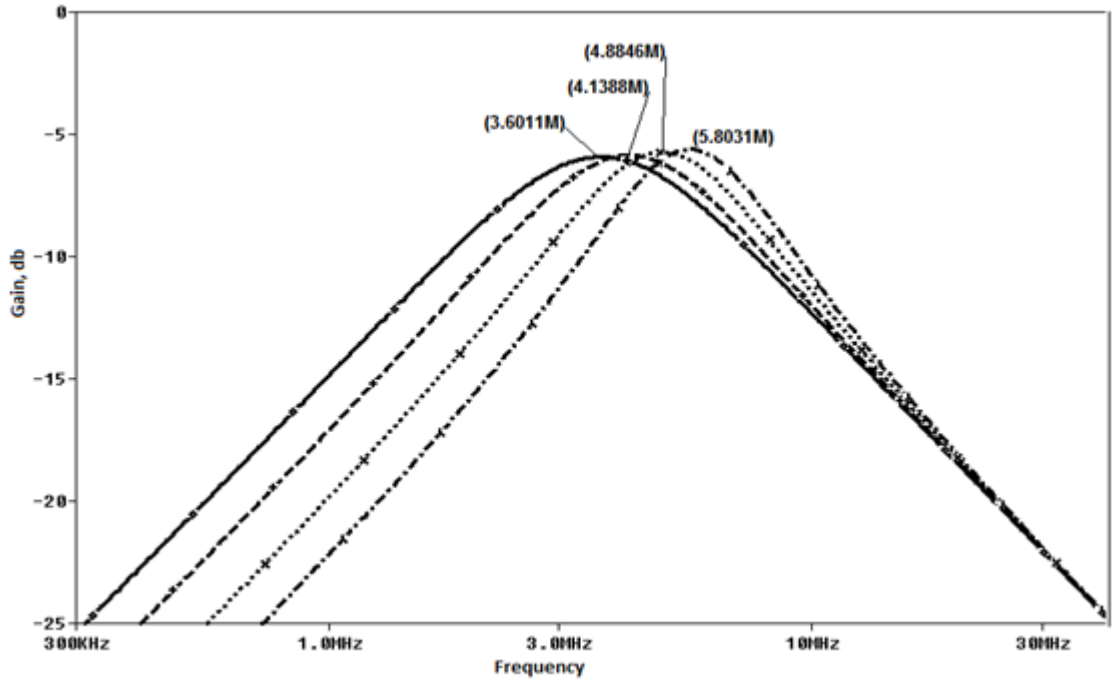

Fig.5.4. Frequency responses of shadow band pass filter with controllable center frequency

5.3. HIGH PASS FILTER WITH CONTROLLABLE BANDWIDTH

5.3.1. CIRCUIT REALIZATION

Figure 5.5 shows a proposed shadow high pass filter obtained by modifying Fig.3.10 of [36]. In Fig.5.5 the external voltage amplifier is built around the circuit of Fig.3.10 from V_o to V_{in2} having gain G and input signal applied to both V_{in1} and V_{in3}.

$V_{in1} = V_{sig}$

$V_{in2} = GV_o$

$V_{in3} = V_{sig}$

Where $G = g_{m6}R_2$

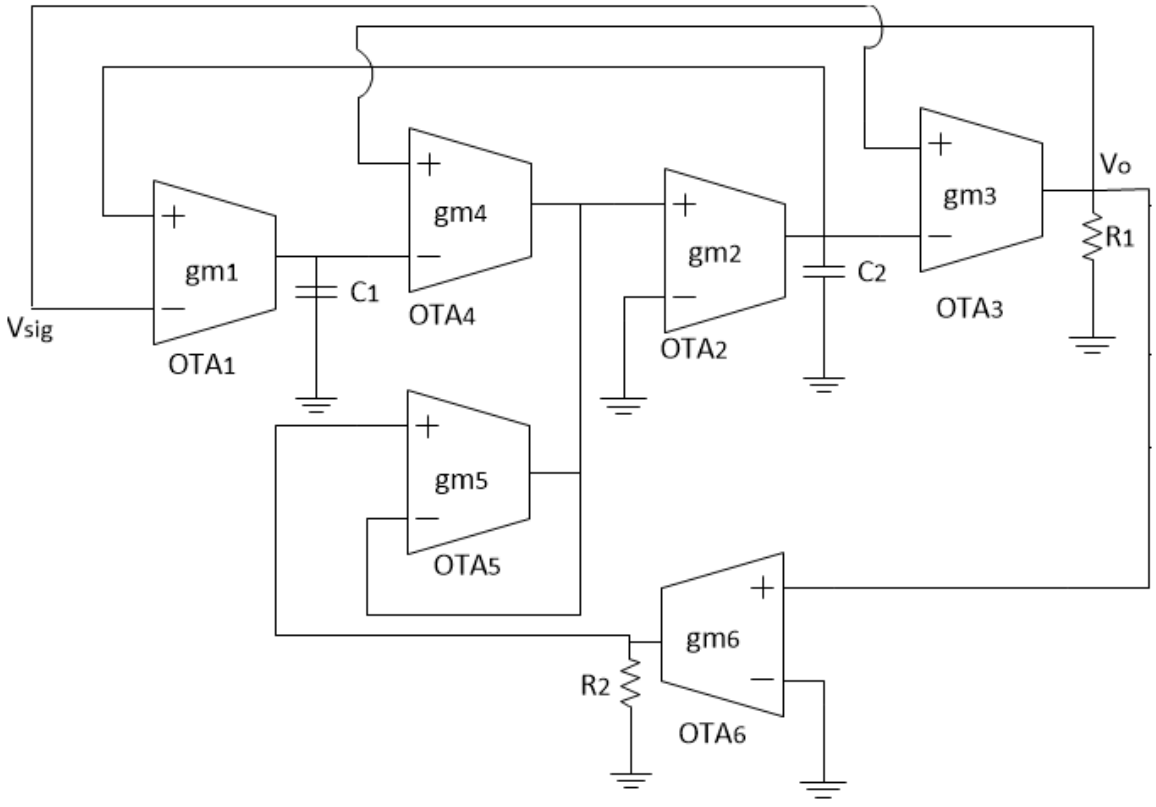

Fig.5.5. OTA-based voltage-mode shadow high pass filter

With the above modifications applied the transfer function of (3.5) can be expressed as

$$V_o = \frac{s^2 R_1 V_{sig}}{s^2 + s\left(\frac{R_1 g_{m2} g_{m3}}{C_2} + G\frac{R_1 g_{m3}}{C_1}\right) + \frac{g_{m1} g_{m2}}{C_1 C_2}} \quad (5.6)$$

Where $G = g_{m6} R_2$

Equation (5.6) is the transfer function of a high pass filter with center frequency and Bandwidth given by

$$\omega_o = \sqrt{\frac{g_{m1} g_{m2}}{C_1 C_2}} \quad (5.7)$$

$$BW = \frac{R_1 g_{m2} g_{m3}}{C_2} + G\frac{R_1 g_{m3}}{C_1} \quad (5.8)$$

Equation (5.8) shows that bandwidth of high pass filter is controlled by the gain G of the external amplifier and the center frequency remains constant.

5.3.2. SIMULATION RESULTS

The SPICE schematics of OTA based high pass filter is shown in Fig.5.6. The high pass shadow filters is verified through SPICE simulators using the circuits of Fig.5.6 with 0.35 µm CMOS process from TSMC. The aspect ratio of transistors in all OTAs of Fig.5.6 are W/L=10µm/1µm for PMOS devices and W/L=5µm/1µm for NMOS devices. The biasing currents for OTA_4 and OTA_5 are fixed as 20µA and the power supplies are given as V_{DD}= -V_{SS}= 1.65 V. Capacitor C_1 and C_2 are of 10pF and the biasing currents I_{abc1}= I_{abc2}= 50µA, I_{abc3}=37µA. Figure 5.9 shows the gain of the shadow high pass filter of Fig.5.6 with C_1 = C_2 = 10pF, R_1 = 10kΩ, R_2 = 5kΩ and for gain =G, 2G, 4G, 8G. The four traces of Fig.5.7 are for the four different values of gain (G, 2G, 4G, 8G). It can be clearly seen that the bandwidth of shadow high pass filter is varying with gain G of the feedback amplifier

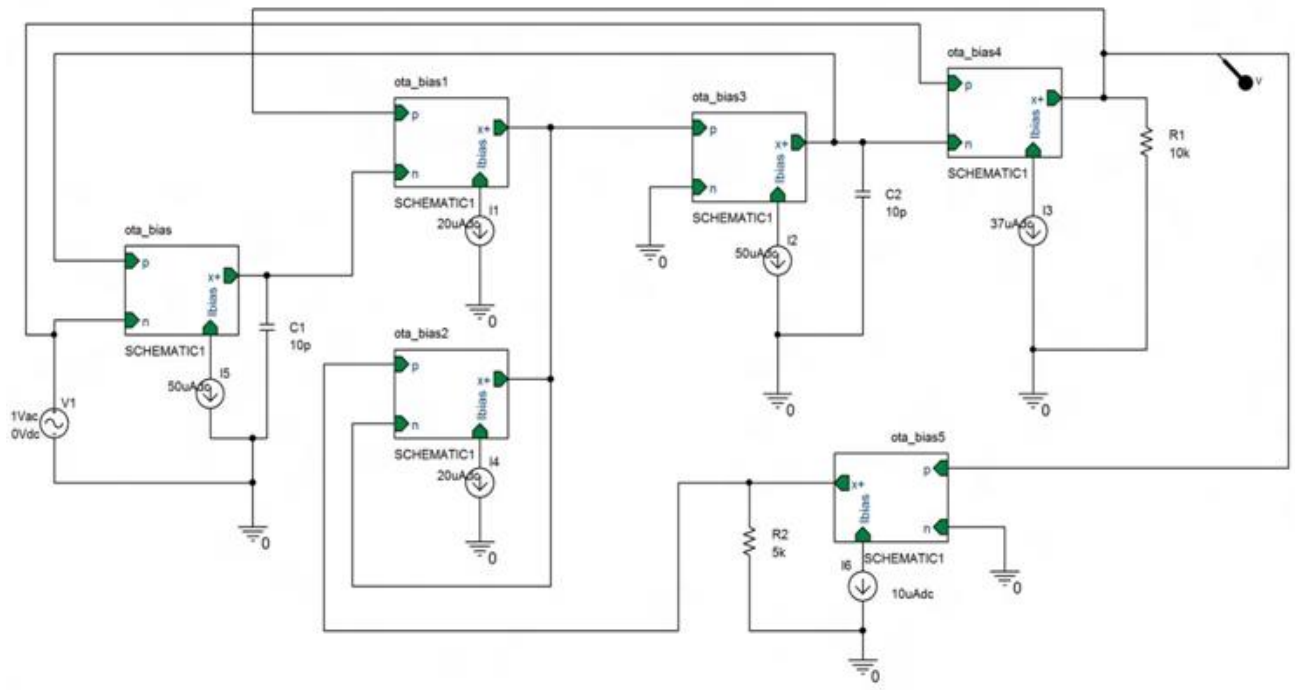

Fig.5.6. SPICE schematic of OTA-based shadow high pass filter

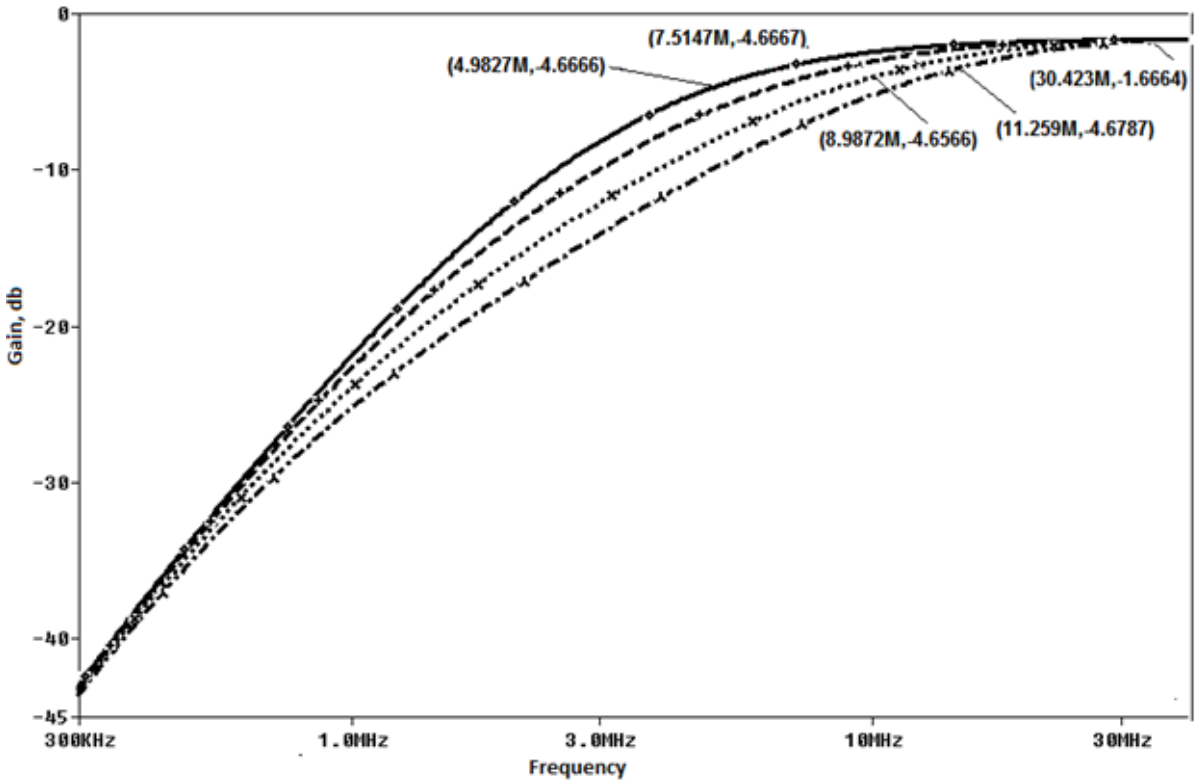

Fig.5.7. Frequency response of shadow high pass filter with controllable bandwidth

The x-axis is the frequency axis where frequency is taken from 300 KHz to 30 MHz on log scale. The plots indicate the gain at y-axis of a high pass filter which shows that the bandwidth of shadow high pass filter is electronically controlled by varying the gain parameter G of the feedback amplifier having value11.25 MHz for gain G, 8.98 MHz for gain 2G, 7.51MHz for gain 4G and 4.98 MHz for gain 8G.

5.4.LOW PASS FILTER WITH CONTROLLABLE BANDWIDTH

5.4.1. CIRCUIT REALIZATION

Figure 5.8 shows a proposed shadow low pass filter obtained by modifying Fig.3.10 of [36]. In Fig.5.8 the external voltage amplifier is built around the circuit of Fig.3.10 from V_o to V_{in2} having gain G and input signal applied to V_{in3} and V_{in1} grounded.

$V_{in1} = 0$

$V_{in2} = GV_o$

$V_{in3} = V_{sig}$

Where $G = g_{m6}R_2$

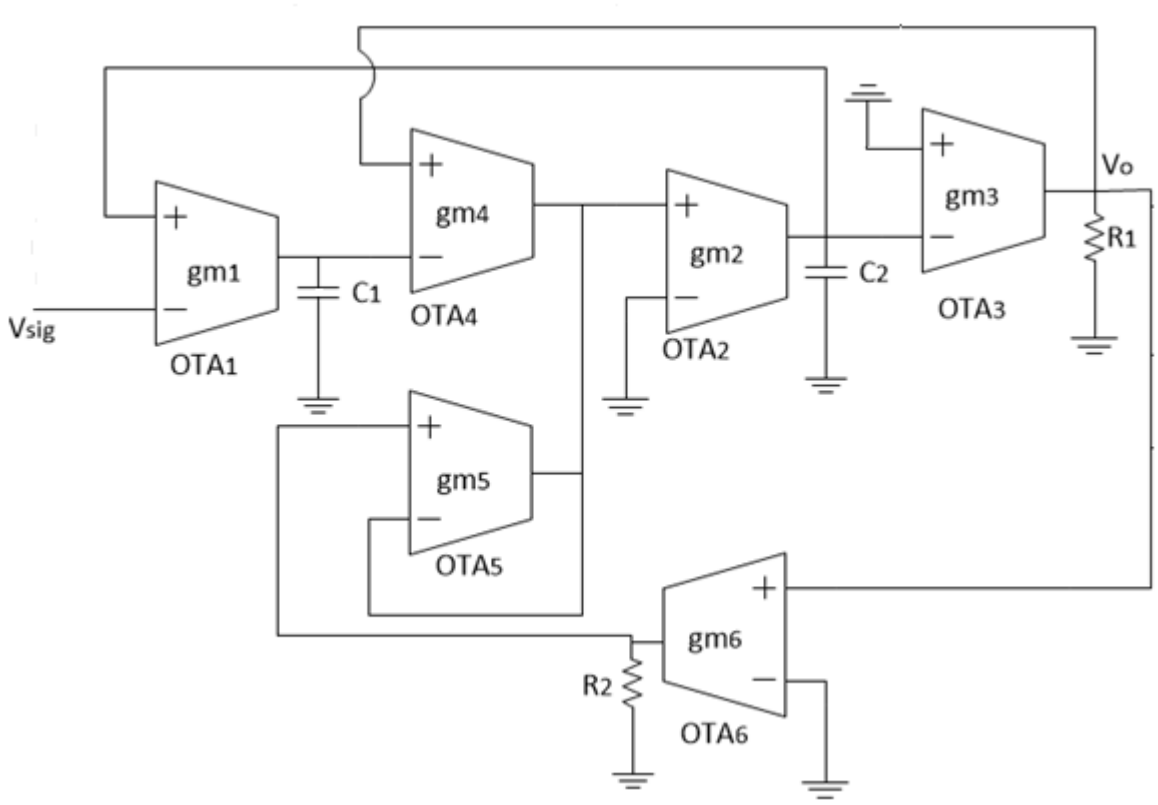

Fig.5.8. OTA-based voltage-mode shadow low pass filter

With the above modifications applied the transfer function of (3.5) can be expressed as

$$V_o = \frac{R_1 \frac{g_{m1}g_{m2}}{C_1C_2} V_{sig}}{s^2 + s\left(\frac{R_1 g_{m2} g_{m3}}{C_2} + G\frac{R_1 g_{m3}}{C_1}\right) + \frac{g_{m1}g_{m2}}{C_1C_2}} \quad (5.9)$$

Where $G = g_{m6}R_2$

Equation (5.9) is the transfer function of a low pass filter with center frequency and Bandwidth given by

$$\omega_o = \sqrt{\frac{g_{m1}g_{m2}}{C_1C_2}} \quad (5.10)$$

$$BW = \frac{R_1 g_{m2} g_{m3}}{C_2} + G\frac{R_1 g_{m3}}{C_1} \quad (5.11)$$

Equation (5.11) shows that bandwidth of high pass filter is controlled by the gain G of the external amplifier and the center frequency remains constant.

5.4.2. SIMULATION RESULTS

The Low pass shadow filters is verified through SPICE simulators using the circuits of Fig. 5.9 with 0.35 µm CMOS process from TSMC. The aspect ratio of transistors in all OTAs of Fig.5.8 are W/L=10µm/1µm for PMOS devices and W/L=5µm/1µm for NMOS devices. The biasing currents for OTA_4 and OTA_5 are fixed as 20µA and the power supplies are given as V_{DD}= -V_{SS}= 1.65 V. Capacitor C_1 and C_2 are of 10pF and the biasing currents I_{abc1}= I_{abc2}= 50µA, I_{abc3}=37µA. Figure 5.10 shows the gain of the shadow low pass filter obtained from Fig.5.9 with $C_1 = C_2 = 10pF$, $R_1 = 10k\Omega$, $R_2 = 5k\Omega$ and for gain G, 2G, 4G, 8G.

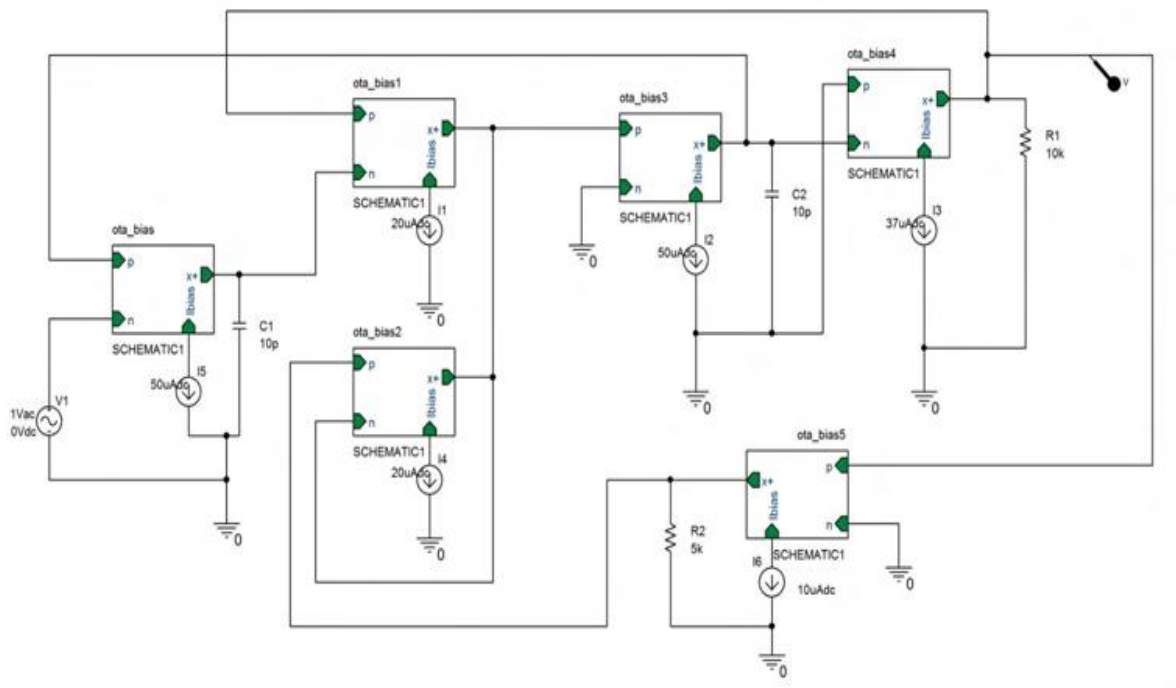

Fig.5.10. SPICE schematic of OTA-based shadow lowpass filter

The four traces of Fig.5.11 are for the four different values of gain (G, 2G, 4G, 8G). It can be clearly seen that the bandwidth of shadow lowpass filter is varying with gain G of the feedback amplifier.

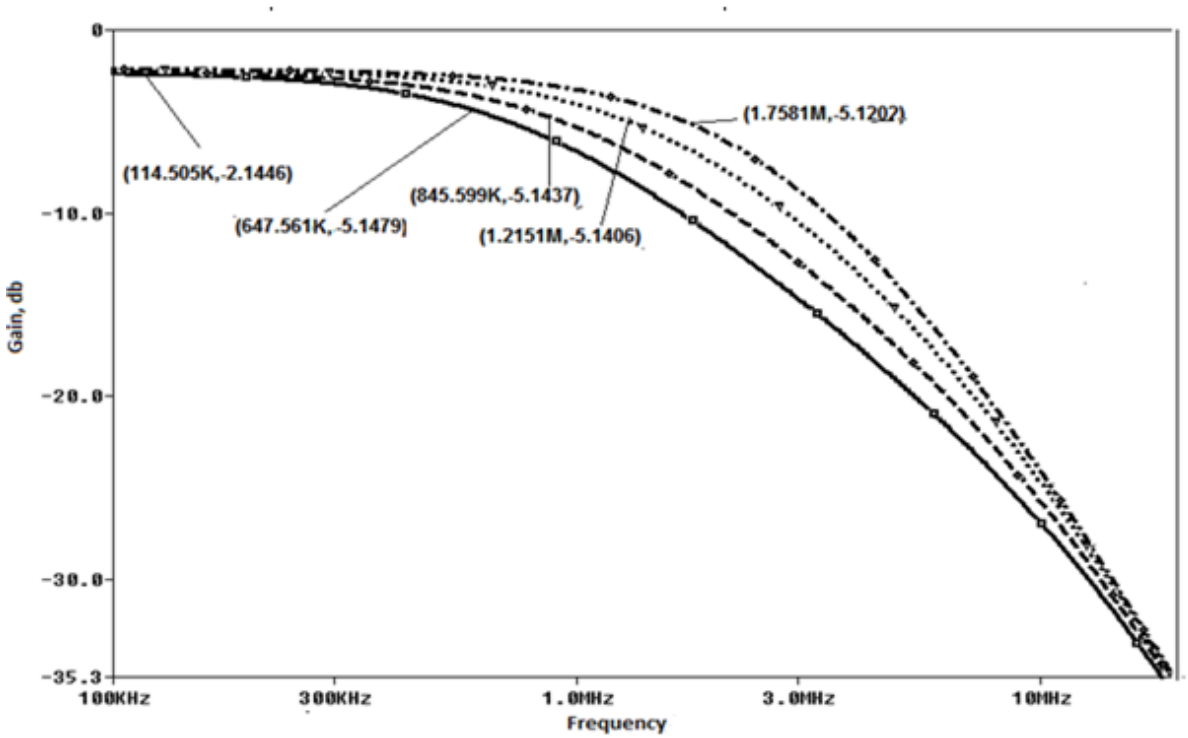

Fig.5.11 Frequency response of shadow low pass filter with controllable bandwidth

The x-axis is the frequency axis where frequency is taken from 100 KHz to 10 MHz on log scale. The plots indicate the gain at y-axis of a low pass filter which shows that the bandwidth of shadow low pass filter is electronically controlled by varying the gain parameter G of the feedback amplifier having value 647.50 KHz for gain G, 845.5 KHz for gain 2G, 1.21 MHz for gain 4G and 1.78 MHz for gain 8G.

5.5.NOTCH FILTER WITH CONTROLLABLE BANDWIDTH

5.5.1. CIRCUIT REALIZATION

Figure 5.12 shows a proposed shadow low pass filter obtained by modifying Fig.3.10. In Fig.5.12 the external voltage amplifier is built around the circuit of Fig.3.10 from V_o to V_{in2} having gain G and input signal applied to V_{in1} and V_{in3} grounded.

$V_{in1} = V_{sig}$

$V_{in2} = GV_o$

$V_{in3} = 0$

Where $G = g_{m6}R_2$

With the above modifications applied the transfer function of (3.5) can be expressed as

$$V_o = \frac{R_1\left(s^2 + \frac{g_{m1}g_{m2}}{C_1C_2}\right)V_{sig}}{s^2 + s\left(\frac{R_1g_{m2}g_{m3}}{C_2} + G\frac{R_1g_{m3}}{C_1}\right) + \left(\frac{g_{m1}g_{m2}}{C_1C_2}\right)} \quad (5.12)$$

Equation (5.12) is the transfer function of a shadow notch filter with Bandwidth given by

$$BW = \frac{R_1g_{m2}g_{m3}}{C_2} + G\frac{R_1g_{m3}}{C_1} \quad (5.13)$$

$$\omega_o = \sqrt{\frac{g_{m1}g_{m2}}{C_1C_2}} \quad (5.14)$$

Equation (5.13) shows that bandwidth of notch filter is controlled by the gain G of the external amplifier and the center frequency remains constant.

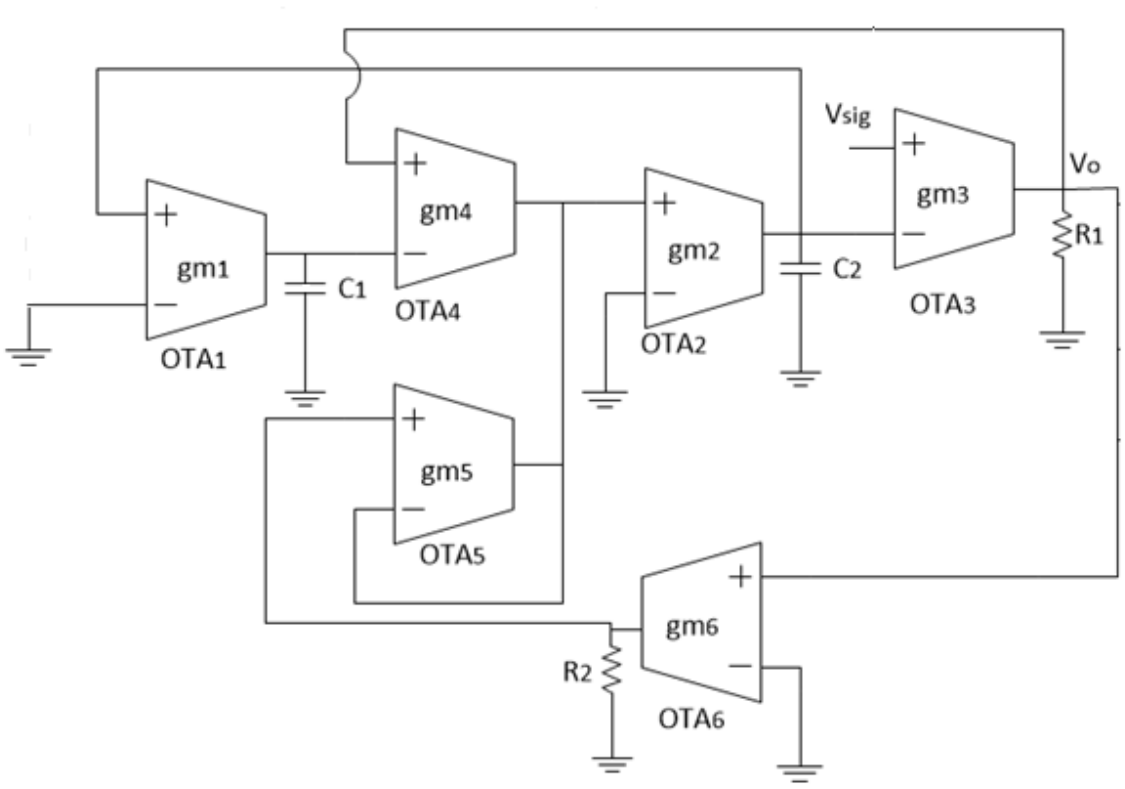

Fig.5.12. OTA-based voltage-mode shadow notch filter with controllable bandwidth

5.5.2. SIMULATION RESULTS

The shadow notch filter is verified through SPICE simulation using the circuit of Fig.5.13 with 0.35 µm CMOS process from TSMC. The aspect ratio of transistors in all OTAs of Fig.5.12 are W/L=10µm/1µm for PMOS devices and W/L=5µm/1µm for NMOS devices. The biasing currents for OTA_4 and OTA_5 are fixed as 20µA and the power supplies are given as V_{DD}= -V_{SS}= 1.65 V. Capacitor C_1 and C_2 are of 10pF and the biasing currents I_{abc1}= I_{abc2}= 50µA, I_{abc3}=37µA. The results shown in Fig.5.14 shows the gain of the shadow notch filter obtained from Fig.5.13 with C1 = C2 = 10pF, R1 = 10kΩ, R2 = 5kΩ, R3 = 5kΩ and gain =G, 2G, 4G, 8G for controllable bandwidth.

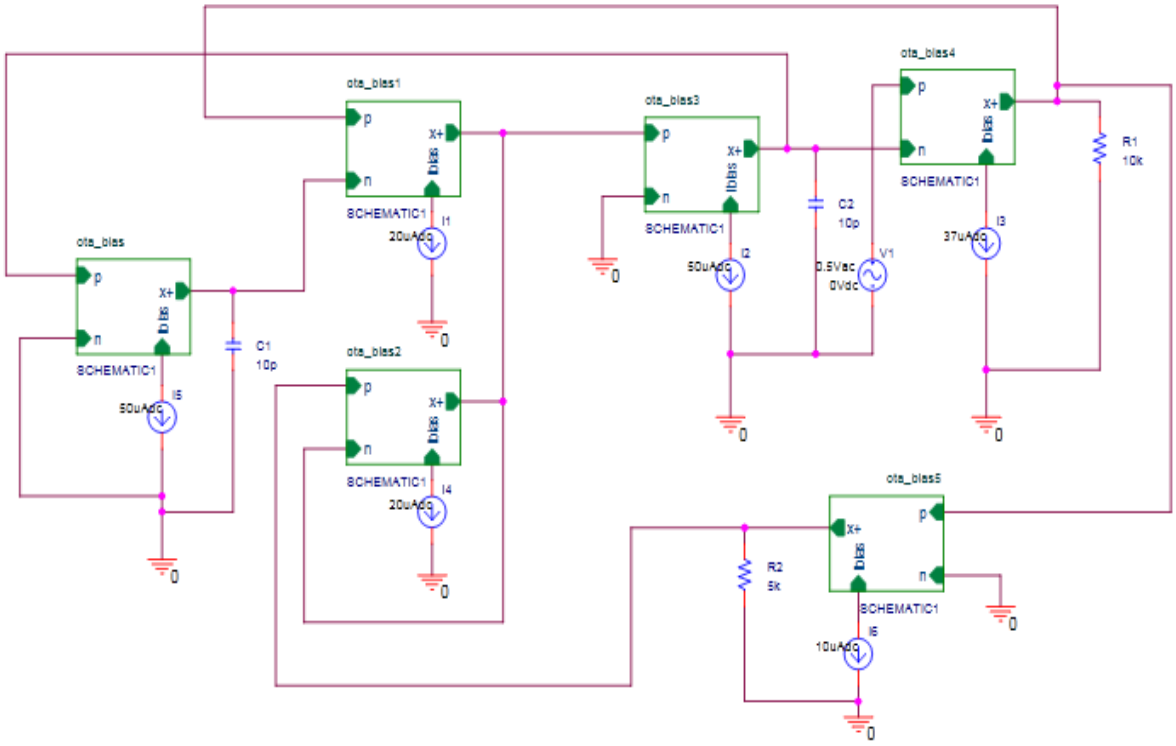

Fig.5.13. SPICE schematic of OTA-based shadow notch filter

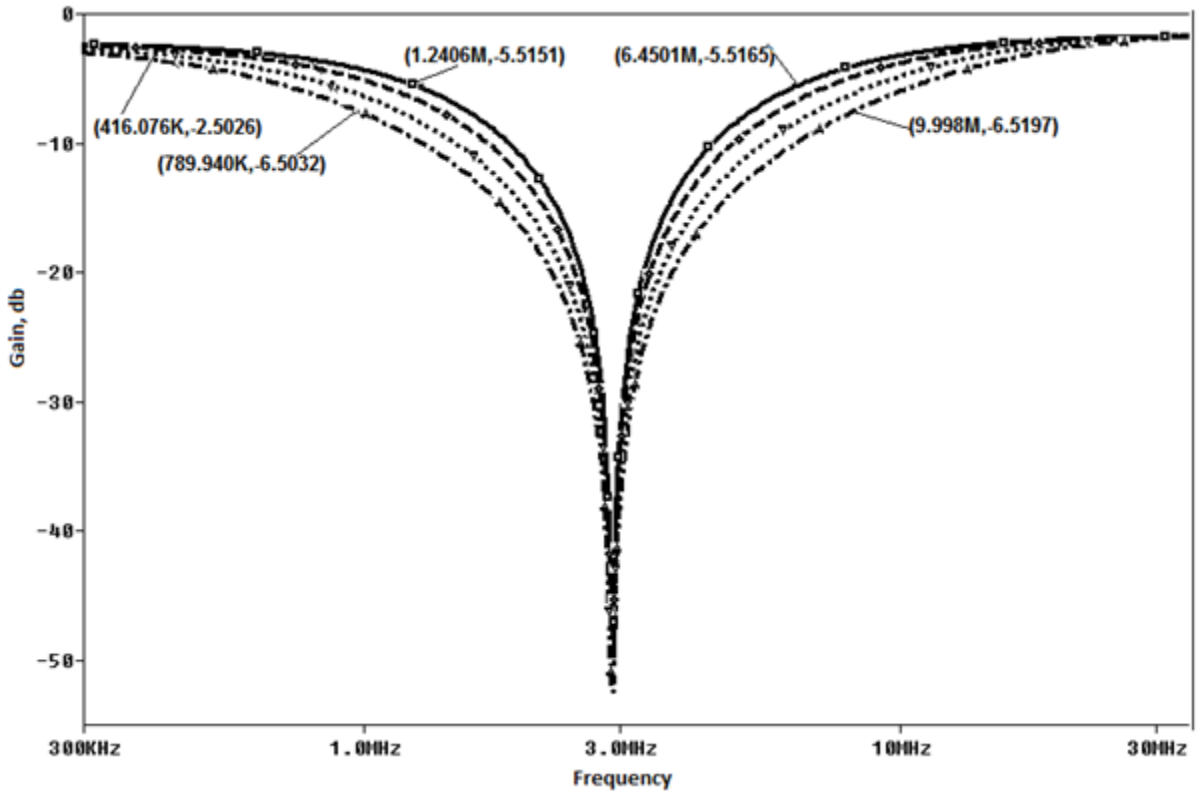

Fig.5.14: Frequency response of shadow notch filter with controllable bandwidth

In Fig.5.14. the x-axis is the frequency axis where frequency is taken from 300 KHz to 30 MHz on log scale. The plots indicate the gain at y-axis of a notch filter which shows that the bandwidth of shadow filter is electronically controlled by varying the gain parameter of feedback amplifier. Figure 5.14 clearly indicates that the BW for gain G is 5.26 MHz and increases with gain having BW 9.2 MHz for gain 8G.

5.6.SUMMARY

In this chapter a new structure of single feedback shadow filter is proposed and also various configurations of single-feedback shadow filters like band pass shadow filter, high pass shadow filter, band pass shadow filter and notch filter are also implemented and simulated to verify the simulation results with the theoretical values. The filter responses are simulated to validate the workability of the proposed filter.

CHAPTER 6

TWO FEEDBACK SHADOW FILTER

The shadow filters can have single feedback or two feedback structures. In this Chapter the two feedback shadow filter structure has been implemented and also shadow notch filter with controllable center frequency and bandwidth is implemented and simulated. The present work uses OTA as an active block for developing the shadow filter circuit.

6.1. PROPOSED OTA SHADOW FILTER USING TWO FEEDBACK

The Block diagram of the two feedback shadow filter structure is shown in Fig.6.1. The shadow filter in Fig.6.1 contrast to the shadow filter presented in [17] does not require summing circuit and also this second-order shadow filter has three inputs and one output rather than one input and two outputs as in [17]. The second-order filter transfer function presented in [29] can be expressed as

$$V_o = \frac{T_1(s)V_{in1} - T_2(s)V_{in2} - T_3(s)V_{in3}}{a_2 s^2 + a_1 s + a_0} \tag{6.1}$$

With $V_{in2} = G_2 V_o$ and $V_{in3} = G_1 V_o$ where G_1 and G_2 are positive real numbers, then the transfer function of the structure of Fig.6.1 can be expressed as

$$V_o = \frac{T_1(s)V_{in1}}{a_2 s^2 + a_1 s + a_0 + G_2 T_2(s) + G_1 T_3(s)} \tag{6.2}$$

The Equation (6.2) clearly indicates that by changing the transfer function $T_1(s)$, $T_2(s)$ and $T_3(s)$ the structure of the filter can be modified to the desired filter such as LPF, BPF and HPF. The center frequency the gain and the bandwidth of the modified filter structure shown in Fig.6.1 can be electronically controlled just by changing external parameters G_1 and G_2 without changing any of the components of second order itself.

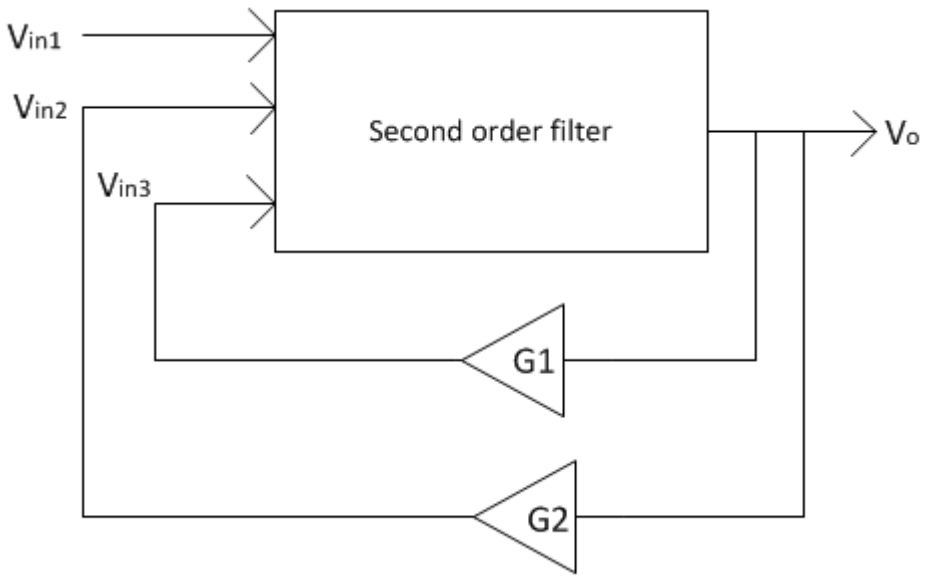

Fig.6.1. Two feedback Shadow filter structure

Let $T_1(s) = s^2 + b_o$, $T_2(s) = b_1 s$ and $T_3(s) = b_2$, then (6.2) after rearranging can be rewritten as

$$V_o = \frac{(s^2 + b_o)V_{in1}}{a_2 s^2 + a_1 s + a_0 + G_2 b_1 s + G_1 b_2} \tag{6.3}$$

The (6.3) can be rearranged as

$$V_o = \frac{(s^2 + b_o)V_{in1}}{a_2 s^2 + (a_1 + G_2 b_1)s + (a_0 + G_1 b_2)} \tag{6.4}$$

Where coefficients $a_2, a_1, a_0, b_2, b_1, b_0$ are constants.

Equation (6.4) shows the transfer function of a second-order band stop voltage-mode filter whose center frequency and bandwidth is given by

$$\omega_o = \sqrt{\frac{a_0 + G_1 b_2}{a_2}} \quad (6.5)$$

$$BW = \frac{(a_1 + G_2 b_1)}{a_2} \quad (6.6)$$

Equation (6.5-6.6) shows that the center frequency can be electronically controlled by adjusting the gain G_1 of the external voltage amplifier of Fig.6.1 without disturbing the bandwidth and the bandwidth can be electronically controlled by adjusting the gain $G_2$of the external voltage amplifier without disturbing the center frequency. Hence center frequency and bandwidth can be independently controlled.

6.2. PROPOSED NOTCH FILTER WITH CONTROLLABLE CENTER FREQUENCY AND BANDWIDTH

6.2.1. CIRCUIT REALIZATION

OTA based shadow notch filter obtained by modifying Fig.3.10 of [36] is shown in Fig.6.2. In Fig.6.2 the two external voltage amplifiers are built around the circuit of Fig.3.10 from V_o to V_{in2} having gain G_1 and V_o to V_{in3} having gain G_2 and input signal applied to V_{in1}.

$V_{in1} = V_{sig}$
$V_{in2} = G_1 V_o$
$V_{in3} = G_2 V_o$

Where G1 is the gain of amplifier consisting OTA6 and G2 is the gain of amplifier consisting OTA7.

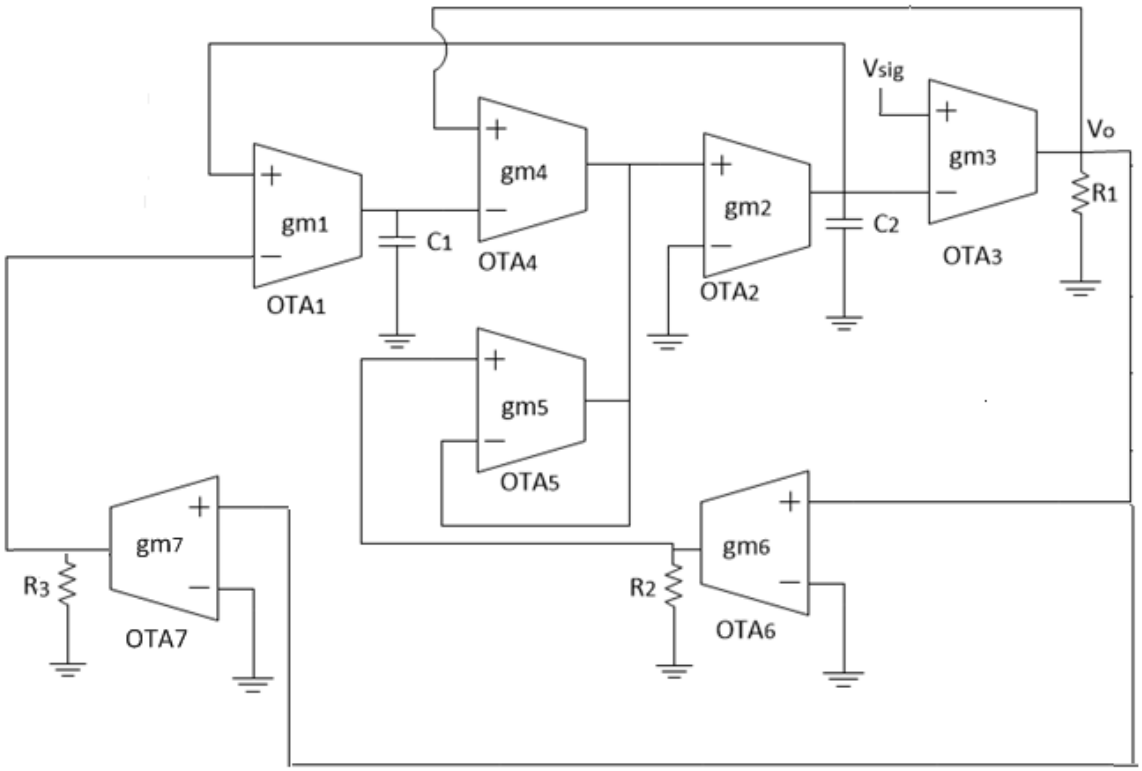

Fig.6.2. OTA-based voltage-mode shadow notch filter

With the above modifications applied the transfer function of (3.5) can be expressed as

$$V_o = \frac{R_1\left(s^2 + \frac{g_{m1}g_{m2}}{C_1C_2}\right)V_{sig}}{s^2 + s\left(\frac{R_1g_{m2}g_{m3}}{C_2} + G_1\frac{R_1g_{m3}}{C_1}\right) + \left(\frac{g_{m1}g_{m2}}{C_1C_2} + G_2\frac{R_1g_{m1}g_{m2}}{C_1C_2}\right)} \quad (6.7)$$

Where $G_1 = g_{m6}R_2$

$G_2 = g_{m7}R_3$

Equation (6.7) is the transfer function of a shadow notch filter with center frequency and Bandwidth given by

$$\omega_o = \sqrt{\frac{g_{m1}g_{m2}}{C_1C_2} + G_2\frac{R_1g_{m1}g_{m2}}{C_1C_2}} \quad (6.8)$$

$$BW = \frac{R_1g_{m2}g_{m3}}{C_2} + G_1\frac{R_1g_{m3}}{C_1} \quad (6.9)$$

Equation (6.8) and (6.9) shows that the center frequency and the bandwidth of notch filter are controlled by the gain G_2 and G_1 of the external amplifier respectively.

6.2.2. SIMULATION RESULTS

The shadow notch filter is verified through SPICE simulators using the circuit of Fig.6.3 with 0.35 µm CMOS process from TSMC. The aspect ratio of transistors in all OTAs of Fig.6.2 are W/L=10µm/1µm for PMOS devices and W/L=5µm/1µm for NMOS devices. The biasing currents for OTA_4 and OTA_5 are fixed as 20µA and the power supplies are given as V_{DD} and V_{SS}= 1.65 V. Capacitor C_1 and C_2 are of 10pF and the biasing currents I_{abc1}= I_{abc2}= 50µA, I_{abc3}=37µA. The results shown in Fig.6.4 and Fig.6.5 shows the gain of the shadow notch filter obtained with C1 = C2 = 10pF, R1 = 10kΩ, R2 = 5kΩ, R3 = 5kΩ and gain =G_1, $2G_1$, $4G_1$, $8G_1$ for controllable bandwidth and gain =G_2, $2G_2$, $4G_2$, $8G_2$ for controllable frequency. The four traces of Fig.6.4 are for the four different values of gain (G_1, $2G_1$, $4G_1$, $8G_1$). It can be clearly seen that the bandwith is varying with gain G_1 of the feedback amplifier. The four traces of Fig.6.5 are for the four different values of gain (G_2, $2G_2$, $4G_2$, $8G_2$). It can be clearly seen that the center frequency is varying with gain G_2 of the feedback amplifier .

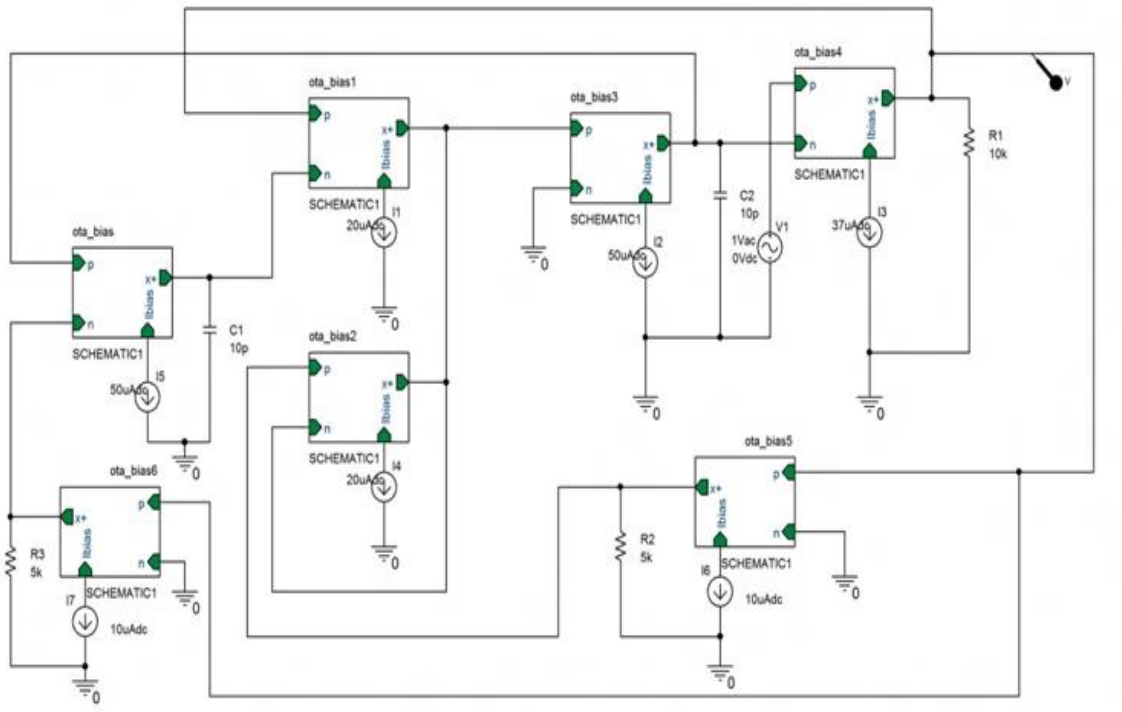

Fig.6.3.SPICE schematic of OTA-based voltage-mode shadow notch filter with two feedback

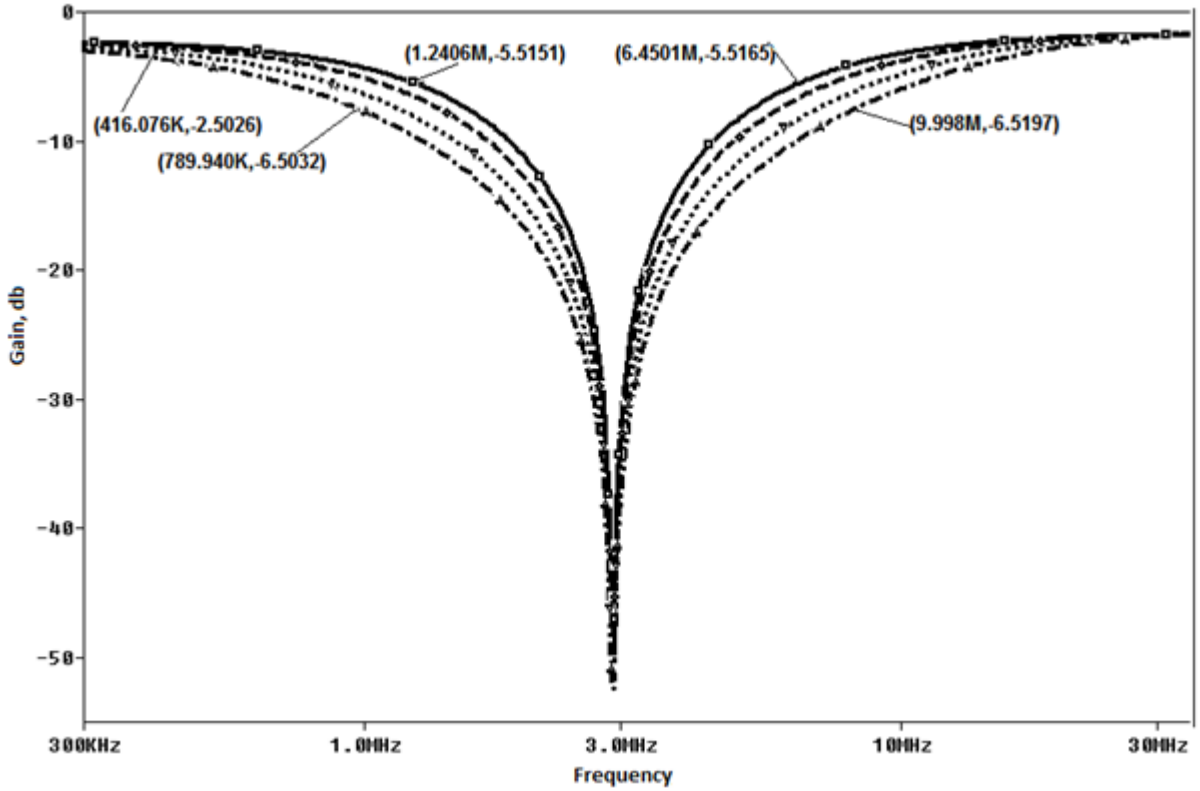

Fig.6.4. Frequency response of shadow notch filter with controllable bandwidth

In Fig.6.4 the x-axis is the frequency axis where frequency is taken from 300 KHz to 30 MHz on log scale. The plots indicate the gain at y-axis of a notch filter which shows that the bandwidth of shadow notch filter is electronically controlled by varying the gain parameter G_1 of feedback amplifier having OTA_6. Figure 6.4 clearly indicates that the BW for gain G_1 is 5.26 MHz and increases with gain having BW 9.2 MHZ for gain $8G_1$.

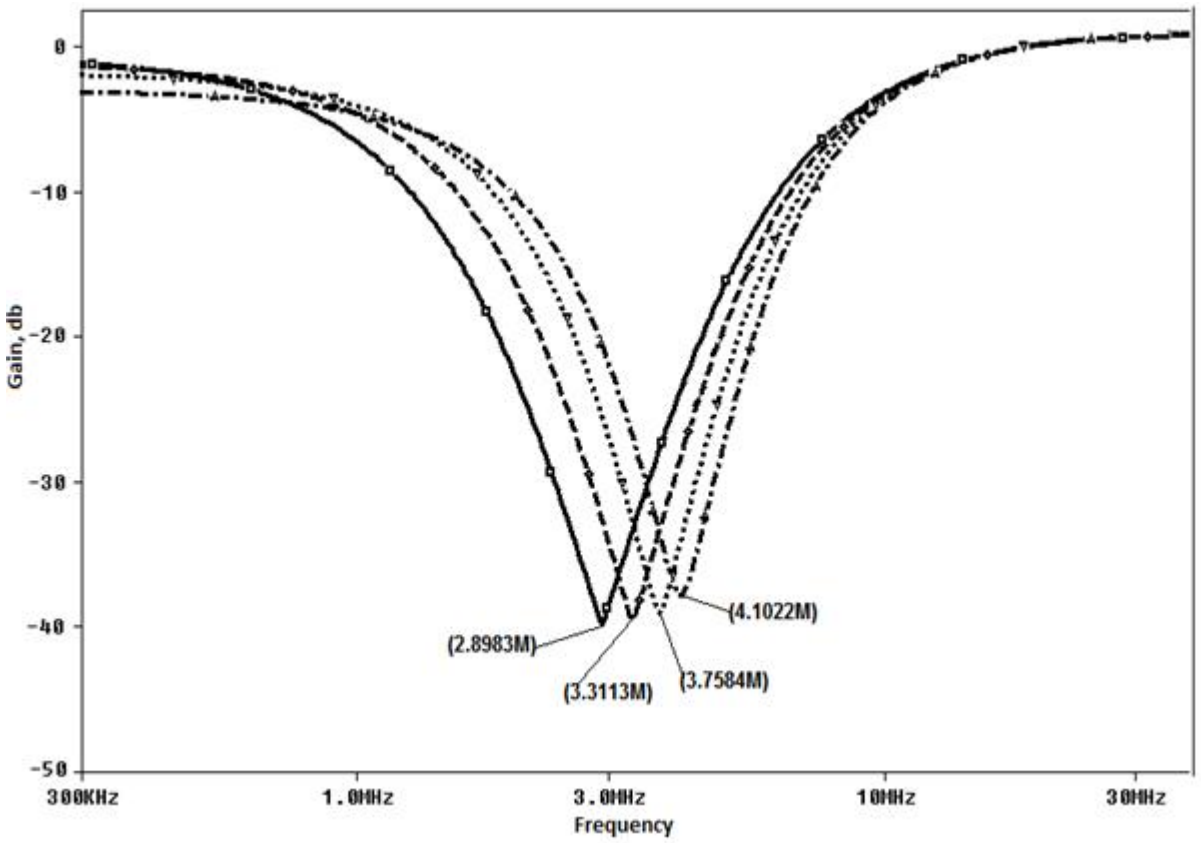

Fig.6.5. Frequency response of shadow notch filter with controllable center frequency

In Fig.6.5 the x-axis is the frequency axis where frequency is taken from 300 KHz to 30 MHz on log scale. The plots indicate the gain at y-axis of a notch filter which shows that the centre frequency of shadow notch filter is electronically controlled by varying the gain parameter G_2 of feedback amplifier having OTA_7.

Figure 6.5 clearly indicates that the centre frequency for gain G_2 is 2.89 MHz, for gain $2G_2$ is 3.31 MHz, for gain $4G_2$ is 3.75 MHz and 4.1 MHZ for gain $8G_2$.

6.3. SUMMARY

In this chapter a new structure of two feedback shadow filter is proposed and also shadow notch filter with controllable center frequency and bandwidth is implemented and simulated. The filter responses are simulated to validate the workability of the proposed filter.

CHAPTER 7

CONCLUSION AND FUTURE WORK

This thesis presents realization of a new OTA based voltage mode shadow filter. In the introductory Chapter a brief on evolution of filters and their importance in electronic circuits has been presented which leads to motivation for the work undertaken. Detailed objective of the work is presented thereafter. The OTA block is realized and characterized in Chapter 2 through SPICE simulations. OTA based applications are realized and simulated in Chapter3 from which it can be concluded that the OTA provides an electronic tuning capability of its trans-conductance gain by adjusting its bias current or voltage and can be implemented by using both bipolar and CMOS technologies also the circuits implemented by using the OTA does not require a resistor which is ideal for any of the integrated circuit implementation. A review of existing literature on design of shadow filter has been presented in Chapter 4.New single feedback voltage mode shadow filter has been proposed in Chapter 5.New voltage-mode implementations of the shadow band pass, high pass, and low pass filters have been presented. In Chapter 6 new two feedback voltage mode shadow filter has been proposed and also new two feedback shadow notch filter implementation have been presented. The proposed voltage mode shadow filter has the following advantages. i) MISO configuration is used which does not require additional summing amplifier. ii) The parameters of this filter can be electronically controlled by adjusting the gains of the external amplifiers easily. iii) While realizing the filter responses, we require no component-matching and also no inverting inputs are required. For validating the responses of proposed filter, it is simulated using 0.35 µm CMOS process from TSMC and the results agree with the theoretical values. The future work includes the generalization of OTA based shadow filter so that any multiple input single output filters can easily converted to the shadow filter without using the summing circuits.

REFERENCES

[1] T. L. Deliyannis, Y. Sun, J. K. Fidler, "**Continuous-Time Active Filter Design**", New York CRC Press LLC, 1999.

[2] M. Kumngern, B. Knobnob, K. Dejhan, "**Electronically tunable high input impedance voltage-mode universal biquadratic filter based on simple CMOS OTAs**", AEU International Journal of Electronics and Communications, vol. 64, pp. 934-939, 2010.

[3] H. P. Chen, S. S. Shen, J.P. Wang, "**Electronically tunable versatile voltage-mode universal filter**", AEU International Journal of Electronics and Communications, vol. 62, pp. 316-319,2008.

[4] M. T. Abuelma'atti, A. Bentrcia, "**A novel mixed-mode OTA-C universal filter**", International Journal of Electronics, vol. 92, pp. 375–383, 2005.

[5] J. Mariem, N. E. Ouazzani, "**Design of an OTA-based microwave active band pass filter**", International Conference on Wireless Technologies, Embedded and Intelligent Systems (WITS), pp. 1-4, 2017.

[6] J. Mariem, EL. Nabih, "**Synthesis of a microwave CMOS active inductor using simple current mirror-based operational Transconductance Amplifier (OTA)**",International Journal of Scientific & Engineering Research, vol. 7, pp. 2229-5518, 2016.

[7] E. Saising, P. Prommee, "**Fully Tunable All-Pass Filter Using OTA and its Application"**, 39th International Conference on Telecommunications and Signal Processing (TSP), pp. 287-290, 2016.

[8] V. Kamat, P.V. Ananda Mohan, K. Gopalakrishna, Dattaguru, "**Novel First-order and Second-Order Current mode filters using dual-output OTAs and Grounded capacitors**", TENCON 2008 IEEE Region 10 Conference, pp. 1-6 , 2008.

[9] M. Kumngern, J. Chanwutitum, "**Voltage-Mode First-Order All pass Filter Using Single-Ended OTAs and Grounded Capacitor**", Second International Conference on Digital Information and Communication Technology and it's Applications (DICTAP), pp. 305-308, 2012.

[10] A.Urbas, J. Osiowski, "**High-frequency realization of C-OTA second-order active filters**", Proc. IEEE Intl. Symp. Circuits Syst, pp. 1106–1109, 1982.

[11] H. Malvar, "**Electronically controlled active-C filters and equalizers with operational transconductance amplifiers**", IEEE Trans. Circuits Syst, vol.31, pp. 645–649 1984.

[12] M. Bhanja, I. Maity, M. S. Roy, Baidyanath Ray, "**A novel Current mode biquadratic OTA-C filter",** IEEE International WIE Conference on Electrical and Computer Engineering (WIECON-ECE), pp. 378-381, 2015.

[13] K. Abdulrahaman, K. Ali, M. Taher, M. T. Abuelma'atti, S. Yunus,"**Digitally programmable integrator and differentiator**", Overseas Publishers Association, vol. 17 pp. 261-268, 1995.

[14] M. Kongpoon, "**Attenuation Technique for Very Low Frequency Filtering using Low-Gm OTA Filters**", International Symposium on Intelligent Signal Processing and Communication Systems, pp. 680-683, 2013.

[15] M. B. Elamien, S. A. Mahmoud, "**Multi-Standard Lowpass Filter for Baseband Chain Using Highly Linear Digitally Programmable OTA**", International Conference on Telecommunications and Signal Processing (TSP), pp. 298-301, 2017.

[16] P. Thongdit, T. Kunto, P. Prommee, "**OTA High Pass Filter-Based Multiphase Sinusoidal Oscillator**", International Conference on Telecommunications and Signal Processing (TSP), pp. 1-5,2015.

[17] Y. Lakys, A. Fabre, "**Shadow filters: New family of second-order filters**", Electronics Letters, vol. 46, pp. 276–277, 2010.

[18] V. Biolkova, D. Biolek, "**Shadow filters for orthogonal modification of characteristic frequency and bandwidth**" Electronics Letters, vol. 46, pp.830–831, 2010.

[19] Y. Lakys, A. Fabre,, "**Shadow filters generalization to nth-class**", Electronics Letters, vol. 46, pp. 985–986, 2010.

[20] S. C. Dutta Roy, "**Shadow filters: A new family of electronically tunable filters**", IETE Journal of Education, vol. 51, pp. 75-78, 2010.

[21] Y. Lakys, A. Fabre, "**A fully active frequency agile filter for multistandard transceivers**", In Proceedings of the international conference on applied electronics, pp. 1-7, 2011.

[22] Y. Lakys, A. Fabre, "**Multistandard transceivers: state of the art and a new versatile implementation for fully active frequency agile filters**", Analog Integrated Circuits and Signal Processing, vol. 74, pp. 63-78, 2013.

[23] Y. Lakys, A. Fabre, "**Encrypted communications: towards very low consumption frequency-hopping active filters**", Analog Integrated Circuits and Signal Processing, vol. 81, pp. 5-16, 2014.

[24] Y. Lakys, B. Godara, A. Fabre, "**Cognitive and encrypted communications: state of the art and a new approach for frequency-agile filters**", Turkish Journal of Electrical Engineering and Computer Science, vol. 19, pp. 251–273, 2011.

[25] N. Pandey, A. Sayal, R. Choudhary, R. Pandey, "**Design of CDTA and VDTA based frequency agile filters**", Advances in Electronics, 2014.

[26] N. Pandey, A. Sayal, R. Choudhary, R. Pandey, M. Tripathi, "**Realization of CDTA based frequency agile filter**", In Proceedings of the IEEE international conference on signal processing, computing and control, pp. 1-6, 2013.

[27] R. Rami, M .Alami, Y. Lakys, B. Delacressonneiere, M. Elbekkali, "**Low power agile active filter with digitally controlled center-frequency**", In Proceedings of the international conference on multimedia computing and systems, pp. 1528–1534, 2014.

[28] S. C. Dutta Roy, "**Shadow Filters – A New Family of Electronically Tunable Filters**" IETE Journal of Education, vol. 51, pp. 75-78, 2010.

[29] M. T. Abuelma'atti, N. Almutairi, "**New current-feedback operational-amplifier based shadow filters**", Analog Integrated Circuit Signal Processing, vol. 86, pp. 471-4802015.

[30] R. Anurag, R. Pandey, N. Pandey, "**OTRA based shadow filters**", Annual IEEE India Conf. (INDICON), pp. 1–4, 2015.

[31] M. T. Abuelma'atti, Naif, R. Almutairi, "**New voltage-mode band pass shadow filter**" 13th Int. Multi-Conf. Systems, Signals & Devices (SSD), pp. 412–415, 2016.

[32] K. Fabian, J. Winai, K. Tomasz , K. Montree, K. David, "**Shadow filter based on DDCC**", IET Circuits Devices & Systems, vol. 11, pp. 631-637, 2017.

[33] M. T. Abuelma'atti, N. Almutairi, "**New CFOA-based shadow band pass filter**", Int. Conf. Electronics, Information, and Communications, pp. 1-3, 2016.

[34] S. Kaehlert, D. Bormann, T. D. Werth, M. D. Wei, L. Liao and S. Heinen, "**Design of Frequency Agile Filters in RF Front end Circuits**", Radio and Wireless Symposium (RWS), pp. 13-16, 2012.

[35] E. Alaybeylu, M. Atasoyu, and H. Kuntman, "**Frequency agile filter structure improved by MOS only technology**", 38th International Conference in Telecommunications and Signal Processing (TSP), pp. 1-5,2015.

[36] N. Wattikornsirikul, M. Kumngern, "**Three-input one-output voltage-mode universal filter using simple OTAs**", Twelth International Conference on ICT and Knowledge Engineering, pp. 28-31, 2014.

[37] P. V. A. Mohan, "**Generation of OTA-C filter structures from active RC filter structures**", IEEE Transactions on Circuits and Systems, vol. 37, pp. 656–660, 1990.

[38] C. M. Chang, "**New multifunction OTA-C biquads**", IEEE Transactions on Circuits and Systems–II, vol. 46, pp. 820–824, 1999.

[39] T. Tsukutani, M. Higashimura, N. Takahashi, Y. Sumi, Y. Fukui, "**Novel voltage-mode biquad without external passive element**", International Journal of Electronics, vol. 88, pp. 13-22, 2001.

[40] J.W. Horng,"**Voltage-mode universal biquadratic filter with one input and five outputs using OTAs**", International Journal of Electronics, vol. 89, pp. 729–737 2002.

[41] M. Kumngern, P. Suwanjan, K. Dejhan, "**Electronically tunable voltage mode universal filter with single-input five-output using simple OTAs**", International Journal of Electronics, vol. 100, pp.1118-1133, 2013.

[42] T. Tsukutani, M. Higashimura, N. Takahashi, Y. Sumi, Y. Fukui, "Voltage-**mode active-only biquad**", International Journal of Electronics, vol. 87,pp. 1435-1442, 2000.

[43] T. Tsukutani, M. Higashimura, N. Takahishi, Y. Sumi, Y. Fukui, "**Versatile voltage-mode active-onlybiquad with lossless and lossyintegrator loop**", International Journal of Electronics, vol. 88, pp. 1093–1101, 2001.

[44] M. T. Abuelma'atti, A. Bentrcia, "**A novel mixed-mode OTA-C universal filter**", International Journal of Electronics, vol. 92, pp. 375–383, 2005.

[45] H. P. Chen, S. S. Shen, J. P. Wang, "**Electronically tunable versatile voltage-mode universal filter**", AEU International Journal of Electronics and Communications, vol. 62, pp. 316-319, 2008.

[46] M. Kumngern, B. Knobnob, K. Dejhan, "**Electronically tunable high input impedance voltage-mode universal biquadratic filter based on simple CMOS OTAs**", AEU International Journal of Electronics and Communications, vol. 64, pp. 934-939, 2010.

[47] S.H. Tu, C.M. Chang, J. N. Ross, M. N. S. Swamy, "**Analytical synthesis of current-mode high-order single-ended-input OTA and equal-capacitor elliptic filter structures with the minimum number of components**", IEEE Transactions on Circuits and Systems-I, vol. 54, pp. 2195-2210, 2007.

[48] R. R. Torrance, T.R. Viswanathan, J.V. Hanson, "**CMOS voltage to current transducers**," IEEE Transactions on Circuits and Systems, vol. 32, pp. 1097-1104, 1985.